Assessing the Influence of Storms on Sea Ice, Snow, and Adélie Penguins along the West Antarctic Peninsula

Mary Elizabeth Stack
Charlottesville, VA

B.S., Boston College, 2017

A Thesis presented to the Graduate Faculty
of the University of Virginia in Candidacy for the Degree of
Master of Science

Department of Environmental Sciences

University of Virginia
April 18, 2023

Committee Members:
Professor Scott C. Doney
Professor Kevin M. Grise
Professor Lauren M. Simkins

Abstract

Polar regions are experiencing some of the most rapid warming due to climate change. The Palmer (PAL) Long-Term Ecological Research (LTER) study area, located along the west Antarctic Peninsula (wAP), is experiencing a shift in the gradient from subpolar to polar ecosystems due to climate change. A shift in the climate gradient impacts sea ice, ocean circulation, ecosystems, and ice-obligate species such as the Adélie penguin. Alongside warming, this region has exhibited increased wind activity, a decrease in the number of sea-ice days, and a decline in the Adélie penguin population. The Adélie penguin is a sentinel of climate change and a key indicator of changes within the ecosystem. It is important to understand how pulse disturbances, in additional to climate shifts, can cause changes in environmental variables. An improved understanding of the influence of storm disturbances is imperative for predictions of species population ecology, habitat changes, and planning for future warming conditions under a changing climate. This study investigates the temporal relationships between storm tracks, sea ice indices, snow, and Adélie penguin chick fledging mass from 1979 to 2021 along the continental shelf of the wAP. Linear regression and linear mixed models are utilized to better understand how storm characteristics relate to variations in sea ice along different subsections of the PAL LTER sampling grid. The sampling area is divided into latitudinal regions (north, south, and far south) as well as into longitudinal zones (coastal, shelf, slope). Differences at the regional and zonal scale in storm and sea ice characteristics occur from 1979 to 2021. Storm frequency showed a statistically significant decrease over time only for the austral winter season. Seasonal sea-ice day of advance shifts later in the season in many areas, especially in coastal zones. Coastal and shelf zones experience a delayed sea-ice advancement when mean storm intensity increases. Increased storm frequency correlates with a later sea-ice retreat day in coastal zones. In addition to these impacts to the Adélie penguin's environment, direct impacts are exhibited in negative correlations between chick fledging mass and storm frequency, intensity, and duration. Seasonal storm characteristics exhibit differences in correlations with CFM, where spring intensity and frequency correlate to a decrease in CFM; whereas summer storm intensity correlates with higher CFM. Future work will seek to distill the complex seasonal differences in storm influence on the chick fledging mass in order to better inform impacts to the Adélie chick survivability.

Acknowledgements

I would like to thank my committee including Scott Doney (chair), Lauren Simkins, and Kevin Grise for their support and guidance in the completion of this research. Thanks also to Megan Cimino for her expert knowledge and help on the Adélie penguin portion of this study. A huge thank you to the support of the Doney Lab members especially Carly LaRoche, Emma Brahmey, Joy Ferenbaugh, Darren McKee, and Olivia Cronin-Golomb. Thanks to Sean Hardison for guidance on data modeling techniques. I would also like to thank my family and friends for supporting me along this journey, especially my sister in science, Maggie.

Table of Contents

1 Introduction

Anthropogenic climate change significantly disrupts ocean climate and marine ecosystems worldwide. According to model predictions, long-term warming in polar regions such as Antarctica, with strong signals along the wAP will continue and accelerate under increased carbon emission scenarios (IPCC 2021). With a high rate of warming, the wAP is a prime study region to evaluate the response of ecosystems under climatic stress. The Palmer (PAL) Long-Term Ecological Research (LTER) study area includes both subpolar and polar conditions. Pulse disturbances, such as storms, may drive abiotic and biotic shifts across the wAP (e.g. species distributions, sea ice dynamics). Understanding drivers of disturbance across temporal and spatial scales along the wAP is crucial for predicting impacts to the local and global ecosystems.

2 Literature Review

2.1 Western Antarctic Peninsula

This study focuses on the PAL LTER study region located along the wAP. The ecosystem experiences seasonal changes due to the annual expansion and retreat of sea ice. In the absence of ice, there is increased wind-ocean mixing, changes to light availability, and fluctuations in the global ocean-atmosphere circulation. Rapid warming has occurred in the wAP since the 1950's with significant declines in sea ice starting in the 1970's (Schofield et al. 2010, Stammerjohn et al. 2012, Ducklow et al. 2013). The PAL study area offers a unique opportunity to study the climate biogeographical shift from a subpolar to polar ecosystem. Subpolar climates in the northern region are characterized by a shorter sea-ice season and a warmer, moister atmosphere; whereas, the southern regions exhibit a more polar climate and have a longer ice season and a cooler, drier atmosphere (Ducklow et al., 2013; Henley et al., 2019; Montes-Hugo et al., 2009; Stammerjohn et al., 2008). PAL is located at the "hinge point" between these subpolar and polar climates of the northern and southern regions (Montes Hugo et al. 2009; Kavanaugh et al. 2015). The transition zone between subpolar and polar climates appears to be shifting southward, meaning that southern regions have become more subpolar (Montes Hugo et al., 2009, Kavanaugh et al., 2015). Therefore, understanding the current ecosystem in the northern regions can be used as an analog to help predict what may occur in the southern regions as climate change persists.

2.2 Sea Ice

The loss of Antarctic sea ice in the future has serious climatic ramifications, including increased CO_2 outgassing during the autumn and winter due to reduced sea ice cover and a weaker vertical ocean stratification in the summer, which would result in a decrease in CO_2 uptake (Shadwick et al., 2021). These would potentially weaken the oceanic CO_2 sink of the Southern Ocean despite any offset from biological activity (Shadwick et al., 2021). Specifically, the Southern Ocean accounts for 40% of the total ocean CO_2 sink (Orr et al., 2001; Fletcher et al., 2006; DeVries, 2014). Sea ice has a high albedo that reflects incoming solar radiation off of the surface instead of being absorbed by darker open water. With less sea ice the albedo effect would decrease, resulting in a positive feedback loop of increased absorption of solar radiation and leading to further warming of the ocean and melting of sea ice. A reduction in sea ice also exposes ice shelves to the open water (Massom et al., 2018), allowing waves to weaken the ice shelves and precondition them for disintegration events (Massom et al., 2018). Models show that sea ice reduces the swells when the concentration of sea ice is moderate to heavy (50-90%) (Massom et al., 2018).

Antarctic sea ice experiences an annual advance-retreat cycle as well as regional and interannual variability (Parkinson & Cavalieri, 2012). Forced by the El Niño Southern Oscillation (ENSO) and Southern Annular Mode (SAM), wind is a significant driver of seasonal sea ice changes in the wAP region (Stammerjohn et al. 2008, Hobbs et al. 2016). Warming ocean temperatures can melt the sea ice faster in the austral spring and summer and delay sea ice advance in the fall. Storm activity can cause sea ice break up (Kohout et al., 2014) or prohibit sea ice from forming. Storm-generated waves maintain enough energy to break up sea ice hundreds of kilometers from the ice edge (Kohout et al., 2014). Retreat [expansion] of sea ice edge correlates with an increase [decrease] in mean significant wave height in the Southern Ocean (Kohout et al., 2014). A 2-meter increase in significant wave height over a decade leads to a 2-degree latitudinal retreat in SIE (Kohout et al., 2014). Understanding changes to Antarctic SIE is crucial to evaluate how the Southern Ocean and global systems may change under continued warming conditions.

The Antarctic SIE across the entire basin exhibited an increasing trend from 1979 to 2014 (Figure 1, Meehl et al., 2019). SIE increased 5 times as quickly during 2000 to 2014 in

comparison to 1979 to 1999 (Meehl et al., 2019). After reaching a record SIE peak in 2014, an unprecedented decrease occurred in 2014 through 2017 and set a new minimum record (Parkinson, 2019). In February 2022, a new SIE minimum was recorded which was 0.17 million km^2 lower than 2017, measured at 1.9 million km^2 (Wang et al., 2022).

Regional Southern Ocean sea ice variations can differ from the basin-scale trends, with often opposing trends in the Ross Sea and Antarctic Peninsula. Since 1979/80, the timing of the seasonal advance and retreat has also shifted, with the wAP decreasing the number of sea-ice days (Figure 2). As of 2010/11, the sea-advance along the wAP happens 2 months later and the retreat occurs 1 month earlier, decreasing the sea ice season by 3 months (Stammerjohn et al., 2012). The wAP and Bellingshausen Sea have seen the most rapid sea ice decrease (Stammerjohn and Maksym, 2017). In 2010, the declining trend in the number of sea ice days per year began to reverse (Schofield et al., 2018). With an increase in sea ice days, there was also a weakening of warming trends (Hobbs et al., 2016). However, the sea ice decline eventually resumed and the trends of warming and sea ice loss continued to be statistically significant (Stammerjohn & Scambos 2020). When the extent and timing of the sea ice season are altered, the repercussions affect species distribution through changes to habitat, food type, light availability, and mixed layer depth (Ducklow et al., 2007, Schultz et al., 2020). Population dynamics across the wAP are highly influenced by sea ice dynamics, including the dynamics of the Adélie penguin population.

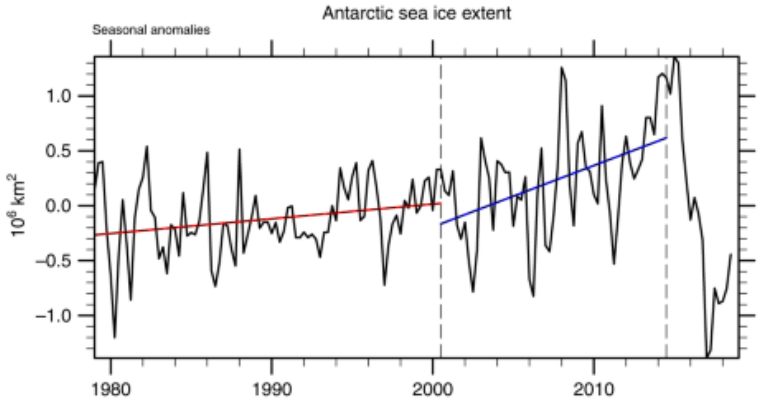

Figure 1. Basin-wide Antarctica sea ice extent from 1979 to August 2018; Trendlines of the seasonal anomalies; Vertical dashed lines indicate beginning and end of the negative IPO (interdecadal Pacific oscillation) period (Figure from Meehl et al., 2019).

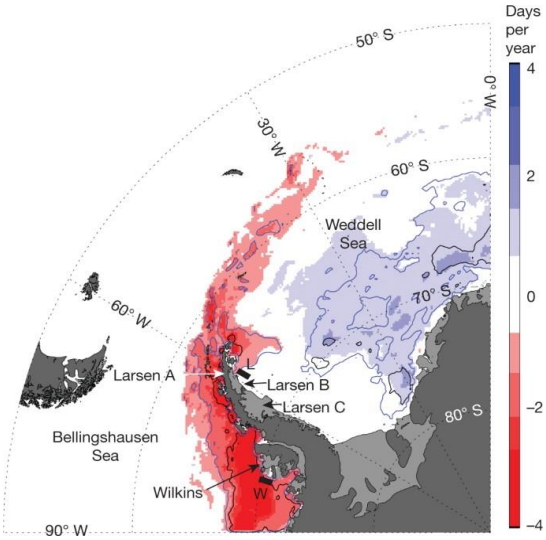

Figure 2. Trend map of satellite-derived annual sea ice season duration for the Weddell, western Antarctic Peninsula and Bellingshausen seas for 1979/1980 to 2009/2010, (Massom et al., 2018).

2.3 Storms & Snow

There is strong regional variability in Antarctic storm intensity, which is measured by wind, ocean waves, and snow accumulation (Hoskins and Hodges, 2005). Over the last decade, Southern Ocean winds and wave height have increased and migrated southward along the wAP (Young et al., 2011, 2017, Young and Ribal, 2019, Reguero et al., 2019). Global climate change and synoptic-scale variability influence Antarctic storm intensity and wind patterns via tropical teleconnections and other climate modes (Yuan et al. 2018, Holland et al. 2019).

Understanding the pulse dynamics of storms is a major question for the PAL LTER group. Pulse events are defined as synoptic storms ranging from a few hours to weeks and the ecological response to them can be short-lived (resiliency), long-lasting, or even irreversible (legacy effect or tipping point) (Palmer LTER NSF Project Summary 2022, Thibault & Brown 2008, Wernberg et al. 2016). Multiple studies have predicted an increase in the frequency of pulse storm events over decadal time scales (Smith 2011, Poloczanska et al. 2013, Harris et al. 2018). Despite this forecast, it has been difficult to hone in on the impacts and ascertain when there might be tipping points in the ocean ecosystem (Gruber et al., 2021; Hienze et al., 2020).

2.4 Adélie Penguins

Adélie penguins (*Pygoscelis adeliae*) are a sentinel of climate change in the wAP region. They are ice-obligate, meaning that they rely on a year-round ice coverage for survival. The

Adélie penguin population near Palmer Station has declined by over 90% since the 1970's, while the ice-intolerant Gentoo penguin population has in turn increased in the study area (Cimino et al., 2016). On Humble Island, the Adélie penguin population declined by 77% from 1991-2016 (Cimino et al., 2019). As changes in Adélie penguin populations occur in the sub-polar northern regions, the impacts observed can be used as an analog for what may happen to the southern colonies which are only recently experiencing population declines (Cimino et al., 2016).

The extent and seasonal timing of retreat of sea ice can impact Adélie penguin populations. If a year exhibits high SIE, it will be followed by a year of higher primary productivity, krill recruitment, and penguin breeding success (Ducklow et al., 2006, Saba et al., 2014, Steinberg et al., 2015, Schofield et al., 2017, Cimino et al., 2019). Alternatively, if there is a low sea ice year, the following year will yield a lower krill recruitment (Saba et al., 2014, Fountain et al., 2016). Antarctic krill (*Euphausia superba*) are a keystone species in the wAP ecosystem. Although there have been population declines farther north (Atkinson et al., 2019), PAL study region has not experienced significant long-term changes in Antarctic krill (Steinberg et al., 2015).

Ecological impacts from storminess include changes in breeding phenology and reproductive success in seabirds (Chappell et al. 1989, Chapman et al 2011, Massom et al. 2008, McClintock et al. 2008, Patterson et al. 2003, Cimino et al. 2019; Fraser et al. 2013). Breeding habitat quality, breeding success, and chick fledging mass (CFM) all are impacted by a shift in precipitation over land caused by storms (Fraser et al. 2013, Cimino et al. 2016, 2014, 2019). Adélie chicks are able to maintain their body temperature over a large range of weather conditions, including low air temperatures and high wind speeds (Chappell et al. 1989); however, survivorship and reduced growth can occur if chicks are continuously exposed to precipitation or intense storms (Muller-Schwarze 1984, Schreiber 2002, Patterson et al. 2003, Olmastroni et al. 2004, Demongin et al. 2010). Parental care can mediate detrimental effects to CFM by providing higher quality and quantity of prey (Chapman et al. 2011). CFM is an indicator of survivability with significantly higher mean CFM (3.152 ± 0.352 kg) for survivors versus non-survivors (3.035 ± 0.258 kg) based on a fledgling resighting study on Humble Island, near Palmer Station (Chapman et al. 2010).

In October, the breeding Adélie penguins return to their colonies on rocky islands, such as Humble Island, to begin nesting (Ainley, 2002). Breeding pairs will lay usually 2 eggs in mid-

November and after an incubation period of 30 to 40 days, the penguin chicks hatch (Ainley, 2002). Once the chicks reach about 20 days of age, they form independent groups away from the nest, known as a crèche (Ainley, 2002). In the austral summer of 2001-2002, multiple storms that hit Palmer Station resulted in a large-scale penguin breeding failure (Massom et al., 2008). Snow accumulation patterns influence the microclimate conditions of nests. Threats to the survivability include snow or meltwater flooding nests, drowning eggs or chicks in nests, or wetting of non-waterproof chick down (Chapman et al., 2011; Massom et al., 2008; McClintok et al., 2008; Boersma et al., 2014). However, these studies classified storms based on local wind and snow deposition, while the interaction between storm frequency or intensity and Adélie penguin ecology has not been explored. Additionally, the krill populations could be impacted by storm disturbances via vertical redistribution which could influence species spatial distribution and food web dynamics. The mechanistic impact of storms on krill abundance and distribution is not well understood. Although investigating this question is not a focus of this study, the importance of krill to penguin foraging and potential relationship with storms are acknowledged.

3 Research Questions and Motivation

A major theme for the Palmer LTER is to investigate drivers of disturbance across temporal and spatial scales. This includes pulse disturbances, such as storms, that may drive changes in the food web across the wAP, including the impact on the declining Adélie penguin population.

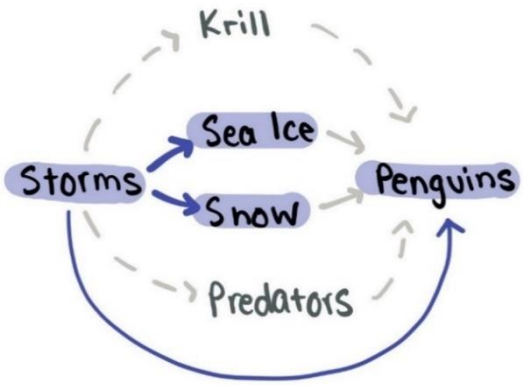

Figure 3. Graphical representation of variables of interest and interconnections (blue). Gray dotted lines represent interactions that are present in the Palmer ecosystem, but will not be explored by this study. The impact of storms on sea ice and snow will be investigated as well as the direct influence of storms on penguin ecology. Krill and predators can impact penguin populations and may be

3.1 Abiotic Drivers: Storms, Sea Ice, and Snow

Based on previous studies, it is known that sea ice and snow are important factors for Adélie penguin population dynamics. Storm track data is able to provide information on individual storms and its movement via coordinates. This study aims to leverage the storm track dataset to assess the impacts that storms have on sea ice, snow, and Adélie penguins (Figure 3). The first step is to investigate the spatial and temporal trends for the abiotic factors of storms, sea ice, and snow.

Q1: On temporal and spatial scales, how are storms changing and what is the impact on other abiotic factors such as sea ice and snow depth?

The goal is to determine if the storms are correlated with either of the other two abiotic metrics that are known influencers on the Adélie population dynamics: sea ice and snow. The research characterized spatial patterns and temporal trends for storm track characteristics (intensity, duration, frequency, and track direction), snow depth, and sea ice indices (advance, retreat, and duration). Storms are expected to increase over time with an increase in storms in the subpolar regions compared to the polar regions. Storm frequency and intensity is expected to be higher in the subpolar compared to the polar regions. Additionally, it is hypothesized that storms of more frequent, intense, and longer duration will cause a delay in sea-ice advance, an earlier sea-ice retreat, a shorter sea ice season duration, and greater snow depth. Sea ice and snow depth are important factors when it comes to Adélie penguin survival. Therefore, it is imperative to investigate the relationships between storms and sea ice as well as snow depth in order to enhance understanding of how Adélie penguins may be impacted by climate change.

3.2 Biotic Response: Adélie Penguins

Once there is an understanding of the interactions amongst the abiotic factors, storms as a physical driver are analyzed with the biotic responses (i.e. chick fledging mass). The goal is to see if storms can be used as a proxy of change to Adélie penguin population dynamics. The next step is to connect the abiotic drivers to the ecology via analysis of correlations between storms and Adélie chick fledging mass (CFM). Thus, the second research question is:

Q2: Do storms have an impact on Adélie penguin chick fledging mass (CFM)? What are the most important storm characteristics in impacting the Adélie penguin CFM?

CFM data were available for a single island (Humble) and therefore spatial relationships will not be explored for this variable. Rather, the focus of this analysis will be on temporal trends and building a model of best fit. It is predicted that fledging mass will be lower when storms are more frequent, intense, and longer in duration. If storms can be a predictor for these penguin metrics, the storm track data can be used as a proxy for changes in penguin ecology that may occur with changing climate conditions.

4 Methods

4.1 Study Site

This study focused on a survey region near the Palmer LTER along the continental shelf of the western Antarctic Peninsula (Figure 4a). The Palmer LTER coordinate system consists of grid and station coordinates that span along and across the continental shelf. The grid area is divided with grid lines 100 km apart across regions: north (600 to 400), south (300 to 200), and far south (100 to -100) with sampling stations 20 km apart across the zones of coast, shelf, and slope (Figure 4b). Palmer Station is located in the northern region of the Palmer LTER study region on Anvers Island (64°46°S, 64°03°W) (Figure 4c). The penguin colony of interest is located at Humble Island, off the south-west coast of Anvers Island in the northern area of the Palmer area (Figure 4c).

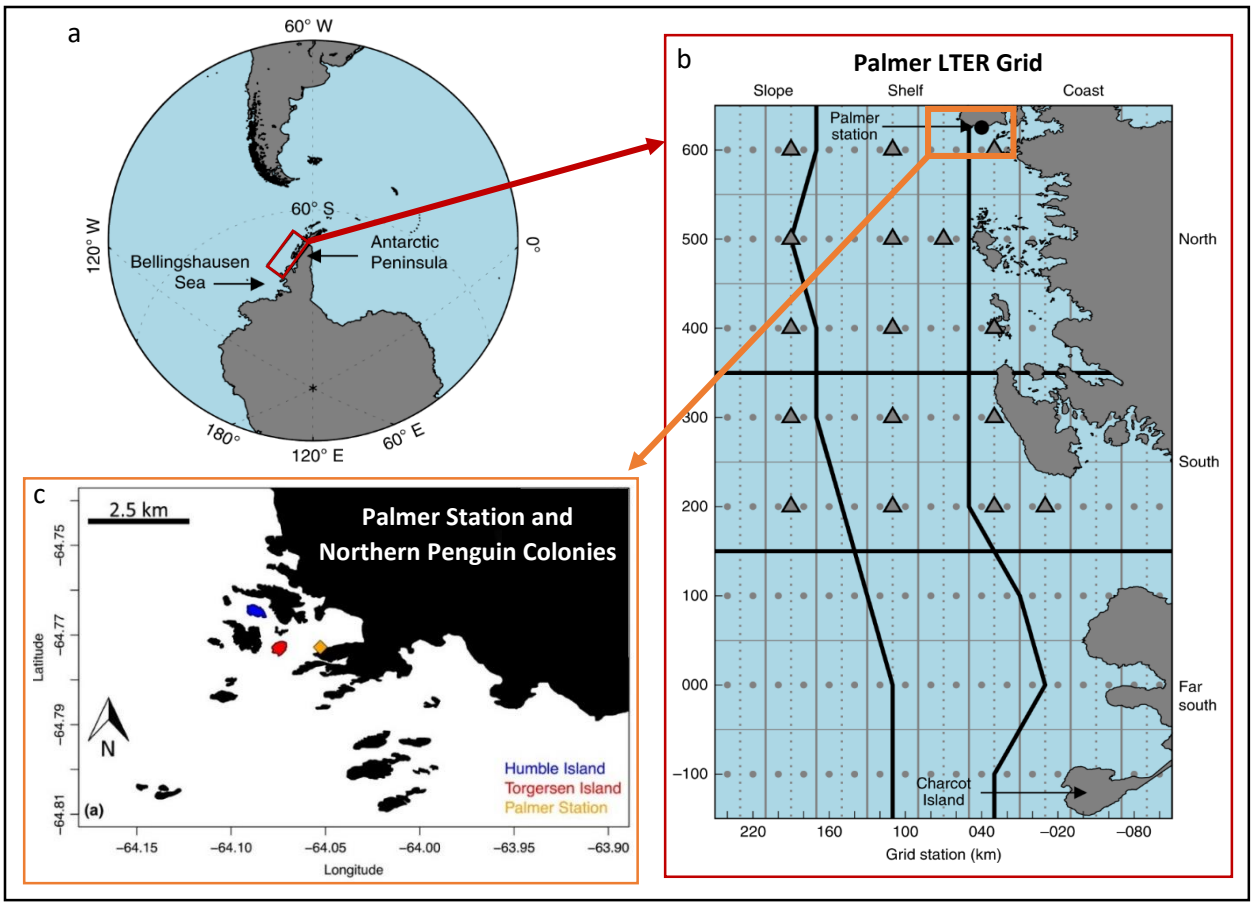

Figure 4. (a) Study site location of Palmer LTER study site along Western Antarctic Peninsula. (b) Study sites are divided into latitudinal regions (north, south, far south) as well as along an offshore longitudinal gradient (coast, shelf, slope); coordinates listed in PAL grid station metrics; dots represent sampling stations. (c) Penguin colony site at Humble Island (blue) and Palmer Station (yellow). Snow depth data was collected from Palmer Station. The gray dots represent sampling stations for other studies at PAL LTER, with a gray triangles denoting sampling stations typically visited each year. Panel a & b modified from Brown et al., 2019, panel c modified from Cimino et al., 2019.

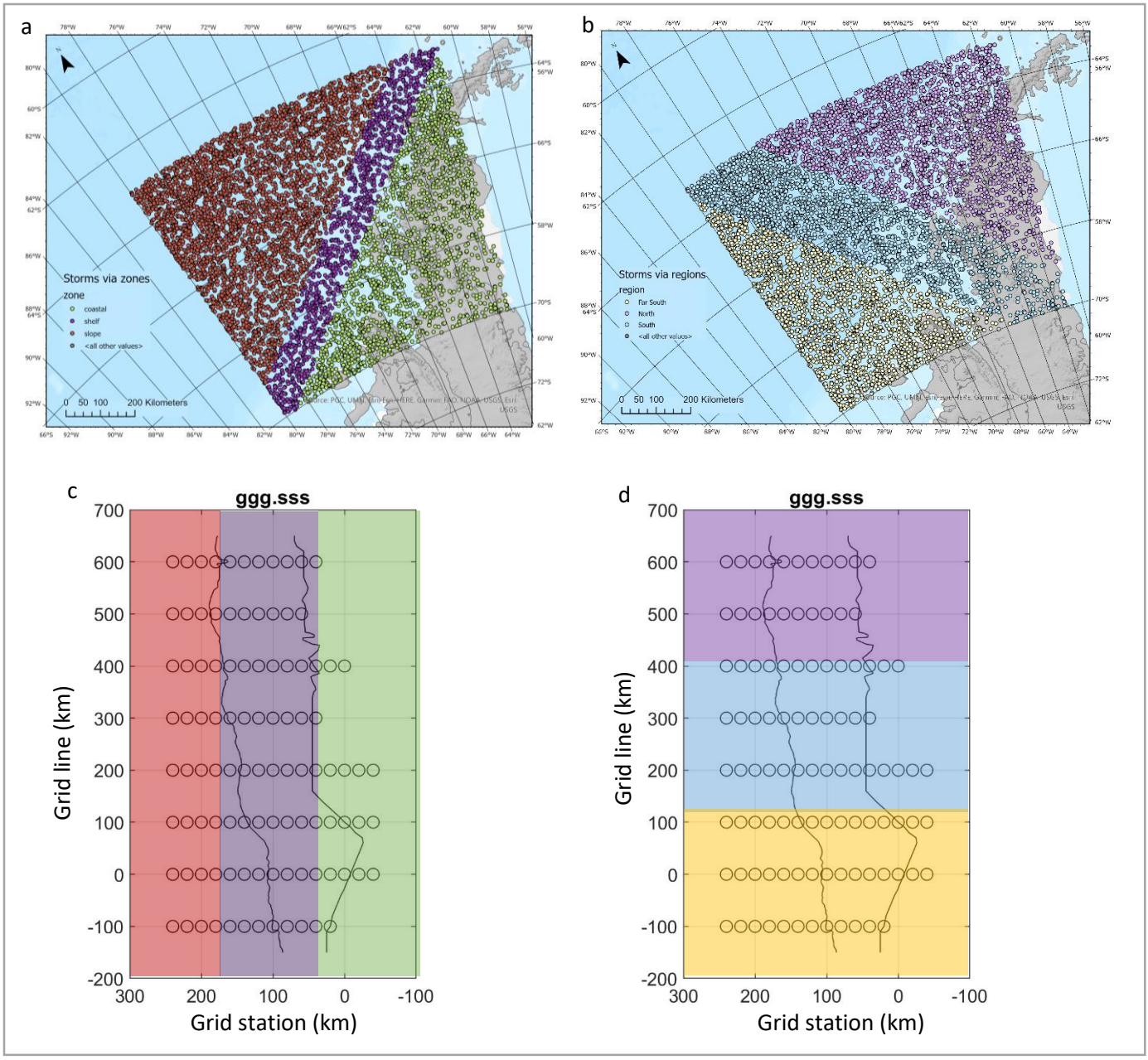

Figure 5. Storm dataset divided into zones (a) and regions (b). These sections are then shown on the grid station panels (ggg.sss) divided into zones (c) and regions (d) which align with map coordinates in Figure 4. For panels c and d, the circles represent sampling stations at PAL LTER and the jagged lines are the divisions between coast, shelf, and slope.

4.2 Datasets

This study compares storm characteristics (frequency, intensity, duration, and track direction) with sea ice indices (advance, retreat, and duration), snow depth, and Adélie chick fledging mass to investigate potential interactions (Table 1).

Storm Tracks

Storm data from 1979 to 2021 (Grise et al., 2014) was provided by Dr. Kevin Grise via Hodges' Lagrangian storm-tracking algorithm (1994, 1995, 1999) utilizing the filtering scheme outlined in Grise et al. (2013). The input data is from relative vorticity from the ERA5 reanalysis (C3S, 2017). Cyclonic Vorticity Units (CVU) is a measure of storm intensity. The algorithm uses relative vorticity to measure the rate of storm rotation (radians per second). The algorithm requires a minimum vorticity of $1.0x10^{-5}s^{-1}$ (hereafter 1 CVU) over the domain of 25ºS-90ºS to verify storm presence. The database is then filtered for cyclones with a minimum lifespan of 2 days, minimum track length of 1000 km, and a minimum peak vorticity of $3.0x10^{-5}s^{-1}$ (3 CVU; Grise et al., 2013). In order to accommodate for comparison of magnitudes, this study utilizes the absolute value to obtain the magnitude of vorticity. The resulting data product contains the magnitude of vorticity (hereafter known as storm intensity), date time recorded, and coordinates. The output is then utilized to determine storm duration, track length, intensity, and direction.

The data were restricted to the Palmer region in order to only include storm tracks that directly passed through the environment. The data were filtered for storms with a center that passes through the PAL LTER grid via mask in Python (-63 > Latitude > -70; -61 > Lon > -80). Most storms in the Southern Ocean have a radius ranging from 500 to 2,000 km (Hoskins & Hodges, 2005; Uotila et al., 2011), therefore the authors acknowledge that storms outside of the grid could influence the PAL ecosystem.

Sea Ice Indices

Sea ice data was obtained from the Palmer LTER EDI Data Portal (Palmer Station Antarctica LTER and S. Stammerjohn, 2021) and was derived from passive microwave satellite data (daily GSFC Bootstrap version 2.0 sea ice concentration). The Palmer full grid area data spans from 1979 to 2016 (provided directly to collaborator Chris Schultz) and the Anvers Island data spans from 1979 to 2021 (doi:10.6073/pasta/0d7bc478d0b40cddf6aefaaab21a545c). The

discrepancy between years is due to the change in classification systems of sea ice indices at Palmer. The sea ice data products no longer include the longitudinal zones of coastal, shelf, and slope. However, when looking at the relationship for sea ice in the region of the Humble Island penguin colony the full length of the dataset is used (1979-2021). The annual ice year is from mid-February to mid-February, i.e. day of year 46 to 410. Sea ice duration is the time elapsed between day of advance and day of retreat within a given sea ice year. Sea ice advance and retreat are defined as the day sea ice concentration was above 15% (advance) or below 15% (retreat) (Stammerjohn, Martinson, Smith, & Iannuzzi, 2008).

Snow Depth

Snow depth from 1990-2020 was obtained via snow stake measurements at Palmer Station (doi:10.6073/pasta/d53c789b7a442f5206f6372f3a356c3d) due to data inaccessibility at Humble Island (Figure 6). Previous studies have suggested that Palmer Station is a close analog for Humble Island snowfall and represents the general trends in the area (Cimino et al. 2019).

Adélie Chick Fledging Mass

Adélie chick fledging mass (CFM) data were obtained from the Palmer LTER EDI Data Portal (doi:10.6073/pasta/875086ecf38755f29f7aa8209e839e7f, Palmer Station Antarctica LTER and M. Cimino, 2022). CFM data span from 1991-2021 and will be compared with the overlapping time period of the storm data (i.e. 1991-2021). The data collection was completed each February when the chicks are considered a fledging and independent of the nest.

Table 1. Variables investigated in this study.

Variable	*Description*	*Unit*
Sea Ice Advance	Day of year of the advancement of sea ice	day of year
Sea Ice Retreat	Day of year of the retreatment of sea ice	day of year
Sea Ice Duration	Ice season duration (days elapsed between adv and ret)	days
Storm Frequency	Number of storms during the year	count
Storm Intensity	Intensity of storm	cyclonic vorticity units (1 CVU = 10^{-5} s^{-1})
Storm Duration	Number of days storm present – calculated from number of days with observation	count (can be converted to hours)
Storm Direction	Direction storm tracks are heading – calculated from coordinates	degrees
Snow Depth	Snow stake depths taken manually at PAL	cm
Chick Fledging Mass	Mass of fledging Adélie chick	gram

4.3 Data Analysis

The analysis was performed in R Studio (version 4.2.1) unless otherwise stated.

Storm Characteristics

Storm characteristics of direction and duration were calculated from the storm track dataset. Storm direction is recorded as the direction the storm is traveling towards. This was calculated for each storm that was recorded more than once in the PAL region in order to find the direction between two points. Direction was calculated for each unique storm using the latitude and longitude input into the 'bearingRhumb' function from the 'geosphere' package. The output in degrees (0-360) was then visualized with wind roses for different temporal and spatial scales, created via the function 'windRose' from the package 'openair'. Duration was calculated by counting the number of times the same storm ID appeared in the defined regional box. For example, if a storm track crossed from shelf to coastal region, it would be counted for each time that it appeared in each regional or zonal box. The tracking algorithm records storms every 6 hours (hours 0, 6, 12, 18). Therefore, the duration can be approximated to have been in the selected spatial box for n counts x 6. For example, if a storm was counted twice, it is considered to have a duration of $\geq$12 hours. Empirical Bayesian kriging (EBK), a geostatistical tool in ArcGIS Pro, was used to interpolate storm intensity for the entire PAL sampling grid across all years (1979-2021). Error is accounted for by estimating the underlying linear semivariogram through repeat simulations.

Chick Fledging Mass

Since there are time periods throughout the year that could impact the adult breeding penguins, models use both the annual average as well as seasonal averages of storm characteristics. The seasonal averages allow for a finer resolution on the impact of storms which occur from chick hatch date to chick fledging date. This time period is crucial in establishing a healthy chick population and storm impact could influence food or habitat availability. Regression analysis and descriptive statistics were used to describe the CFM over time. The storm and CFM were analyzed for any correlations via linear regression and further explored with appropriate statistical techniques dependent on if distribution and residuals were normal (e.g. linear mixed model versus generalized linear mixed model). Linear regression with each predictor variable is explored for collinearity before utilizing the parameter in models [Eq. 2].

There are confounding factors that could influence the CFM, potentially resulting in a greater amount of unexplained variance. Therefore, analysis must be conducted with caution and acknowledgement of these unaccounted-for effects.

Descriptive Statistics

Descriptive statistics were used to determine mean and standard deviation of each variable (storm characteristics, sea ice indices, snow depth, and CFM) and on spatial scales (full PAL LTER grid area, region subsites, zone subsites) for storms and sea ice data. The 'sumtable' function in the 'vtable' package was used to perform a test of independence between variables. The test performed was a group F-test with ANOVA for numeric variables and a chi-squared test for categorical variables. A Tukey HSD (Honestly Significant Difference) test was also used when comparing if groups (e.g. seasons, regions, zones) were significantly different from one another (Eq. 1).

$$HSD = M_1 - M_2 / (\sqrt{(MS_w [1/n])}) \qquad [Eq. 1]$$

Equation 1. Tukey Post Hoc HSD Test where *HSD* is the Honestly Significant Difference, M_1 and M_2 are mean values, MS_w is mean square width and n is number per mean.

Linear Regression

Linear regression analysis (Eq. 2) was performed on spatial scales (full PAL LTER grid area, region subsites, zone subsites) and temporal scales (annual, seasonal, monthly) for each physical driver (storms, sea ice, snow) to investigate if there were temporal trends. Storms were also looked at for correlations with sea ice indices and snow depth. Simple and multiple linear regression (Eq. 2, Eq. 3) were used to determine if the independent variable (i.e. storm intensity, frequency, duration, direction) could predict the dependent variable (i.e. sea-ice advance, retreat, duration; and snow depth). An alpha level of 0.05 is used for determining statistical significance.

$$Y = B_0 + B_1X + e \qquad [Eq. 2]$$

Equation 2. Simple linear regression model where Y is the dependent variable, B_0 is the intercept, B_1 is the regression coefficient, x is the independent variable, and e is the error of the estimate.

$$Y = B_0 + B_1X_1 + B_2X_2 + B_3X_3 + e \qquad [Eq. 3]$$

Equation 3. Multiple linear regression model where Y is the dependent variable, B_0 is the intercept, B_1 is the regression coefficient for X_1, X_1 is the first independent variable explaining variance in Y, B_2 is the regression coefficient for X_2, X_2 is the second independent variable, B_3 is the regression coefficient for X_3, X_3 is the third independent variable, and e is the error of the estimate.

Linear Mixed Models

Linear mixed models are used to investigate the best method for predicting CFM based on frequency, intensity, duration and direction of storms [Eq. 4]. Models are validated via checking residuals and fit of modeled data to the observed. The 'stepAIC' function from the 'MASS' package in R was used to determine the model with the lowest AIC (Akaike information criterion) and considered the model of best fit. AIC is used to determine model performance when removing or adding predictors. Model equations are included in the results section for each model run. Validation of the models is completed using the DHARMa package which uses a simulation-based approach to create residuals for linear mixed models and test for over-dispersion, outliers, and autocorrelation.

$$R_i = X_i \times \beta + Z_i \times b_i + \varepsilon_i \qquad [Eq.\ 4]$$

Equation 4. Linear mixed effects model (Zuur et al., 2009) where R_i is the dependent response variable at year i, $X_i \times \beta$ is the fixed term, $Z_i \times b_i$ is the random term, ε_i is the error of the estimate.

Table 2. Illustration of Sea Ice Season for example year 2009-2010 SI Season. Seasons are written as the austral season (i.e. for southern hemisphere). 'Storms' lists the months that a storm could potentially have an impact on the SI. 'Effects' lists possibilities for how storms would impact the sea ice indices.

Sea Ice Season	2009-2010 SI Season												2010-2011 SI Season *(not fully pictured)*					
Ex Yr	2009											2010						
Mon	F	M	A	M	J	J	A	S	O	N	D	J	F	M	A	M	J	J	A
Season	Sum	Fall			Winter			Spring			Summer			Fall			Winter		
Sea Ice	Ret	Advance						Retreat						Advance					

Storms	-	Summer storms (DJF) Fall storms (MAM) Winter storms (JJA)	Winter storms (JJA) Spring storms (SON) Summer storms (DJF)	Summer storms (DJF) Fall storms (MAM) Winter storms (JJA)
Effects	-	Storms might delay advance (lateral effects, cooling water, break up sea ice)	Storms could encourage retreat (break up sea ice) and lateral ice transport	Storms might delay advance (lateral effects, cooling water, break up sea ice)

5 Results

Some results do not have a significant p-value ($p < 0.05$), but are retained in this portion for discussion purposes. Statistical significance is shown via * for $p<0.1$ (not significant, but notable), ** for $p<0.05$ (significant), and *** for $p<0.01$ (highly significant). Additional graphs and tables can be found in the supplemental material.

5.1 Storms

Storm Frequency

Temporal differences in storm frequency were explored on annual, seasonal, and monthly scales. Annual frequency was also investigated for any spatial differences in temporal trends (Table 3, Table 4). The annual and monthly average frequency demonstrate both inter-annual and intra-annual variability (Fig. 6). The annual frequency of storms does not show a statistically significant change over time (Fig. 6). Storms still did not show any significant temporal changes when subdivided into regions (north, south, far south) (Table 3, Fig. S1) and zones (coastal, shelf, slope) (Table 3, Fig. S2). However, when divided into each sub-site – consisting of both a region and zone – the south coastal sub-site exhibited a significant decrease over time (slope = -0.0923 storms/year, $p < 0.05$) (Table 4, Fig. 7). When investigating seasonal differences, winter storms showed a significant decrease in the frequency (slope = - 0.0959 storms/year, $p < 0.05$) (Table 5, Fig. 6). However, no month exhibited a statistically significant ($p < 0.05$) relationship between number of storms and years (Fig. S3, Table S1).

Storm Intensity

The distribution of storm intensity appears Gaussian with a positive skew with most storm intensities are between 2.5 to 5 ($10^{-5}s^{-1}$ or CVU). The mean storm intensity did not have a linear trend over time, however winter storm intensity showed a significant increase in CVU, albeit a small increase (0.008 CVU/year) (Table 6). Storm intensity was investigated at the

regional, zonal, and region-zone scale. In all of those analyses, only north coastal has a significant increase in storm intensity, also very small (0.00982 $\pm$ 4.36e-3, n=718, R^2=7.05e-3, p=0.0245). There is variability throughout the dataset with outliers in many of the years (Fig. 8). The median (black bar) shifts around from year to year, there are some years that are often significantly different from other years such as 1990, 1997, 2001, and 2011 (Table S2). Storm intensity by season exhibits differences with a dip in storm intensity in January followed by increased variability leading up to austral winter months (Fig. 8). Results from a Tukey HSD test showed that most months are different from each other (Table S3). Seasonal variability (Table 6, Fig. 8) appears to be similar to the annual variability (Fig. 8). When analyzing storm intensity spatially and seasonally, the significant trends are predominantly during the winter and fall seasons (Table 7). On average, storm intensity appears to decrease as storms move inland, with slope having the highest intensity and coastal areas having the lowest in all regions (Fig. 8). Storm intensity is significantly different in the south and north regions (Fig. 8) and is concentrated area along the slope in the northern section of the Palmer LTER (Fig. 8).

Storm Duration

Storm duration is how long each individual storm lasted in a spatial area. The average duration over the entire study period (1979-2021) is 1.6 +/- 1.1 counts, which equates to approximately 9.6 hours +/- 6.6 hours. The average duration per month does not change drastically, however there are differences between months (Table S4). There are no significant seasonal trends in duration over time (Table 8).

Storm Direction

The average direction storms moved towards for the entire study period (1979-2021) was 115^o (or ESE). Significant differences were found between the direction of storms in the summer with all other seasons (Table 9). The spatial analysis showed a difference in storm direction in the South and North with the Far South as well as between coastal and shelf with slope (Table 10). The direction of storms specifically within the northern region were investigated on a monthly scale due to this area being the location of the penguin colony of interest on Humble Island (Fig 11). Wind roses display both storm direction and intensity with the percentage of storms moving in a direction depicted by size of the wedge (Fig. 9, 10, 11).

Interactions Among Storm Characteristics

Interactions between storms were investigated to determine if more intense storms tend to last longer or happen less frequently. Storm characteristics were also tested for collinearity in order to determine which variables could be used in models. Correlations among storm characteristics (frequency, intensity, duration, and direction) were looked at for all data (Fig. S5) as well as by season (Fig. S6), region (Fig. S7) and zone (Fig. S8). Storm characteristics for the annual means in the northern region did not show any significant ($p<0.05$) correlations (Fig. S9). Correlation values were less than 0.3 for all variables (frequency, intensity, duration, direction). Regional (Table 11) and zonal (Table 12) differences are statistically significant for storm intensity, bearing, and duration, meaning that the spatial differences are significant across the PAL LTER grid.

Storm Figures and Tables

Fig 6. Frequency of storms in PAL LTER grid area over study period from 1979-2021. (a) Annual frequency of storms over study period; green line represents the linear trend ($p > 0.05$, Table 4) and the gray area represents the 95% confidence interval around the linear trend. (b) Average frequency per month $\pm$ 1 standard deviation. (c) Seasonal frequency of storms over study period divided into seasons: winter, spring, summer, and fall; green line represents the linear trend and the gray area represents the 95% confidence interval. Only winter frequency of storms is significantly ($p<0.05$) with a temporal decrease at about -0.0959 storms per year.

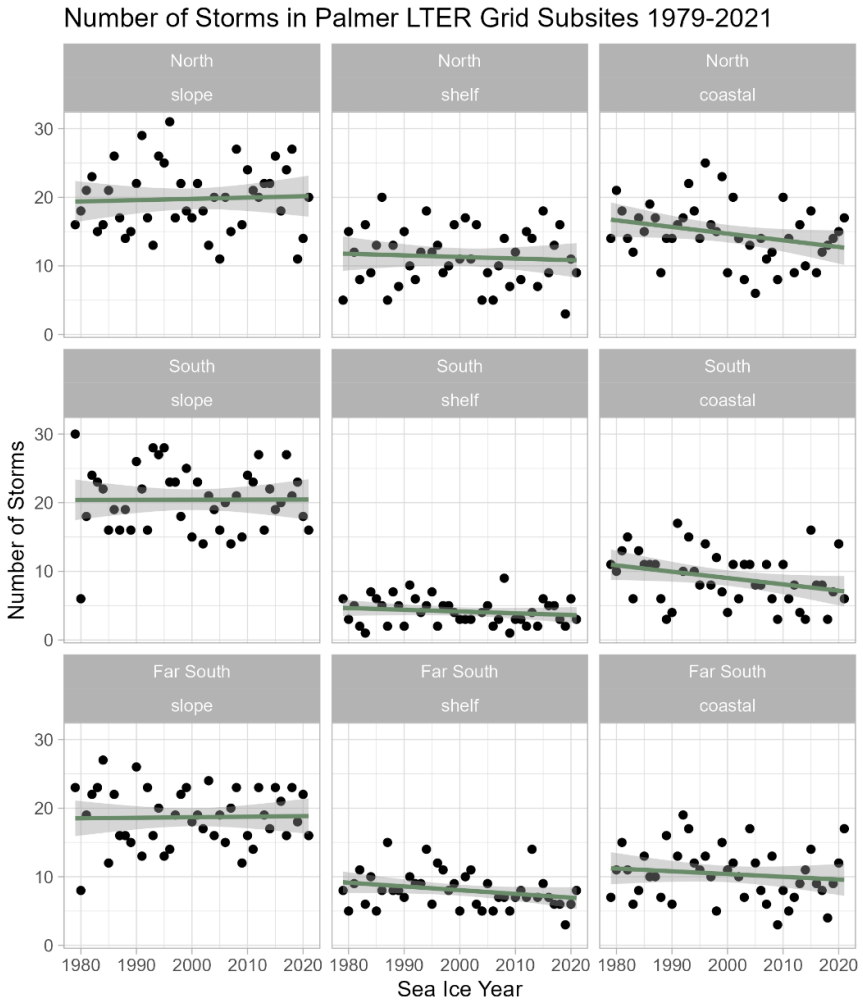

Fig 7. Number of storms in Palmer region from 1979 to 2021 divided into sub-sites (regions and zones). The south coastal sub-site exhibited a significant decrease over time (slope = -0.0923 storms/year, $p = 0.046$) (Table 5).

Table 3. Frequency of storms per year on various spatial scales from 1979-2021. Statistical significance shown via *p<0.1, **p<0.05, ***p<0.01. Slope is the number of storms/year. SE is the standard error of the slope. N = 43 years.

Area	*Mean*	*SD*	*Slope*	*SE*	*R^2*	*P-value*	*Signif*
PAL	61.2	8.19279	- 0.1105	0.1004	0.0287	0.277	
North	35	6.99	- 0.0826	0.0859	0.0220	0.342	
South	29.9	5.88	- 0.0699	0.0723	0.0223	0.339	
Far South	29.0	4.33	- 0.0829	0.0522	0.0579	0.120	
Coastal	29	7.14	- 0.154	0.0855	0.0731	0.0796	*
Shelf	21.9	5.25	- 0.102	0.0634	0.0599	0.114	
Slope	43.4	6.70	0.0116	0.0833	0.000475	0.890	

Table 4. Frequency of storms per year for each sub-site (region-zone) from 1979-2021. Statistical significance shown via *p<0.1, **p<0.05, ***p<0.01. Slope is the number of storms/year. N= 43 (years).

Area	*mean*	*Stdev*	*Slope*	*SE*	*R^2*	*P-value*
North-coastal	14.7	4.27	- 0.0971	5.09e-2	8.16e-2	0.063*
North-shelf	11.3	4.09	- 0.0231	5.08e-2	5.03e-3	0.651
North-slope	19.8	4.88	0.0187	6.07e-2	2.32e-3	0.759
South-coastal	**9.02**	**3.79**	**- 0.0923**	**4.49e-2**	**9.35e-2**	**0.046****
South-shelf	4.14	1.95	- 0.0253	2.39e-2	2.74e-2	0.295
South-slope	20.4	4.82	0.00121	5.99e-2	9.92e-6	0.948
Far South-coastal	10.4	3.84	-0.0400	4.73e-2	1.72e-2	0.400
Far South-shelf	8.05	2.64	- 0.0545	3.17e-2	6.74e-2	0.093*
Far South-slope	18.7	4.22	- 0.00785	5.25e-2	5.45e-4	0.882

Table 5. Seasonal frequency of storms and correlation with time from 1979-2021. Statistical significance shown via *p<0.1, **p<0.05, ***p<0.01. Slope is the number of storms/year. R^2 value is the adjusted R^2.

Season	*Mean*	*SD*	*Slope*	*SE slope*	*R^2*	*P-value*
Winter	16.5	3.98	- 0.0959	0.472	0.0916	0.049**
Spring	16.4	4.5	- 0.0593	0.0552	0.0274	0.288
Summer	13.4	4.28	0.0284	0.0530	0.00695	0.595
Fall	15.2	3.06	0.0201	0.0379	0.00679	0.599

Table 6. Seasonal intensity of storms and correlation with time from 1979-2021. Statistical significance shown via *p<0.1, **p<0.05, ***p<0.01. Slope is number of storms/year.

Season	*Mean*	*SD*	*Slope*	*SE*	*R2*	*P-value*	*Signif*
Winter	**4.09**	**1.59**	**0.008**	**0.00331**	**0.00405**	**0.01253**	**
Spring	3.92	1.56	-0.0003	0.00314	0.000007	0.9119	
Summer	3.41	1.36	-0.0019	0.00271	0.000325	0.4748	
Fall	4.04	1.63	0.003	0.00331	0.000686	0.3029	

Table 7. Spatial & seasonal intensity of storms and correlation with time from 1979-2021. Statistical significance shown via *p<0.1, **p<0.05, ***p<0.01. Slope is number of storms/year.

Season	*Region*	*Zone*	*Mean*	*SD*	*Slope*	*SE*	*R2*	*P-value*	*Signif*
Winter	**North**	**Coastal**	**3.71**	**1.51**	**0.0193555583**	**0.008701872**	**2.550949e-02**	**0.027312000**	**
Spring	**North**	**Slope**	**3.85**	**1.61**	**0.0148940388**	**0.007274105**	**1.396581e-02**	**0.041487276**	**
Fall	**North**	**Slope**	**4.23**	**1.61**	**-0.0166574354**	**0.007665570**	**1.618670e-02**	**0.030596698**	**
Winter	**South**	**Shelf**	**3.28**	**1.14**	**0.0297708312**	**0.013280146**	**9.848934e-02**	**0.029842749**	**
Winter	**South**	**Slope**	**4.41**	**1.73**	**0.0217066134**	**0.008757439**	**2.249255e-02**	**0.013806339**	**
Fall	**South**	**Shelf**	**3.88**	**1.57**	**0.0430301067**	**0.019895168**	**1.096091e-01**	**0.036911285**	**
Fall	**Far South**	**Slope**	**4.26**	**1.61**	**0.0201787234**	**0.0077**	**2.561324e-02**	**0.009742488**	***

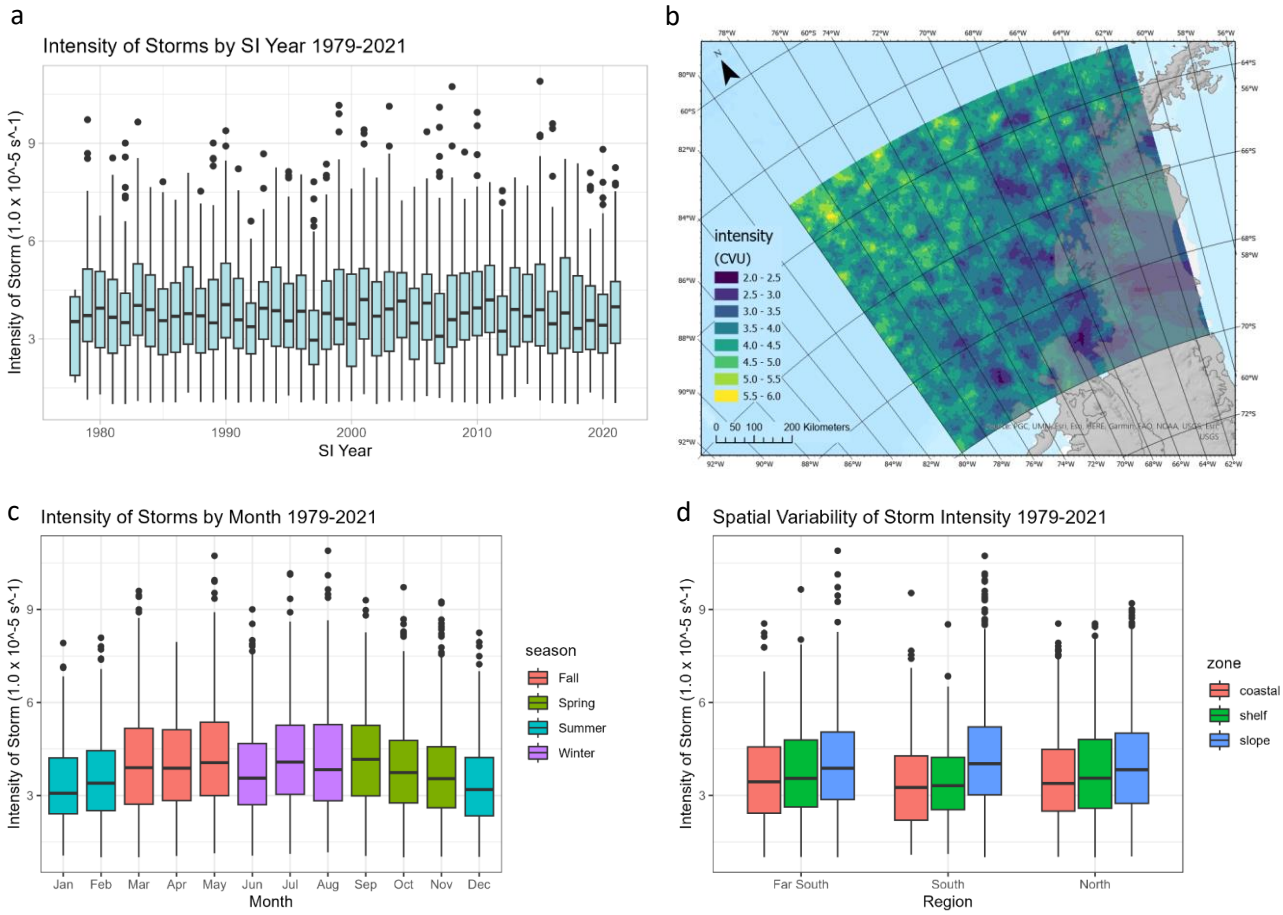

Figure 8. Storm intensity in the PAL LTER grid from 1979-2021. Boxplot (a, c, d) tails represent maximum value in the data, 75th [or 25th] percentile + [-] 1.5 x Interquartile Range. (a) Annual variability of storm intensity. (b) Density map of all storm intensities measured in CVU at Palmer LTER sampling sites along the Western Antarctic Peninsula. (c) Seasonal and monthly variability of storm intensity. (d) Spatial variability (by zone and region) of storm intensity. Storm intensity is significantly different in the south and north regions.

Table 8. Seasonal duration of storms and correlation with time from 1979-2021. Statistical significance shown via *p<0.1, **p<0.05, ***p<0.01. Slope is number of storms/year.

Season	*Mean*	*SD*	*Slope*	*SE*	*R2*	*P-value*	*Signif.*
Winter	1.44	0.87	0.0006836	0.00180	0.0000935	0.7047	
Spring	1.52	1.04	0.0038	0.00208	0.00207	0.0646	*
Summer	1.88	1.45	-0.0039	0.00290	0.00117	0.175	
Fall	1.57	1.00	-0.00294	0.00204	0.00134	0.1498	

Table 9. Seasonal differences in direction of storms from 1979-2021. Statistical significance shown via *p<0.1, **p<0.05, ***p<0.01. Subscripts with the same letter represent statistically similar means and different letters represent statistically different means.

Season	*Mean*	*Stdev*	*Slope*	*P-value*	*SE*	*R2*	*Tukey HSD Significance*
Winter [a]	110	80	0.12	0.5761	0.22	3.76e-4	Summer***
Spring [a]	116	63	0.01	0.9713	0.17	1.37e-6	Summer**
Summer [b]	125	68	-0.50	0.0028	0.17	8.92e-3	Spring**, Fall***, Winter***
Fall [a]	108	65	0.22	0.2152	0.17	1.72e-3	Summer**

Table 10. Spatial differences in direction of storms from 1979-2021. Analysis was not looked at the differences mixing region (north, south, far south) with zone (coastal, shelf, slope). Tukey HSD test results show statistical significance shown via *p<0.1, **p<0.05, ***p<0.01. Subscripts with the same letter represent statistically similar means and different letters represent statistically different means. The number subscript represents which means were compared to each other (e.g. a^1 compared with b^1).

Area	*Mean*	*Stdev*	*Tukey HSD Significance*
North [a1]	121	56.5	Far South***
South [a1]	121	69.7	Far South***
Far South [b1]	107	74.2	North***, South***
Coastal [a2]	106	97.8	Slope***
Shelf [a2]	109	77.3	Slope**
Slope [b2]	119	57.8	Coastal***, Shelf**

Fig. 9. Temporal difference in storm direction and strength (CVU) from 1979-2021. Four plots show various breakdowns: (a) all storms over time period, (b) seasonal, (c) monthly, and (d, next page) annual. Mean storm strength is shown in the bottom right.

(a) Frequency of counts by storm direction (%)

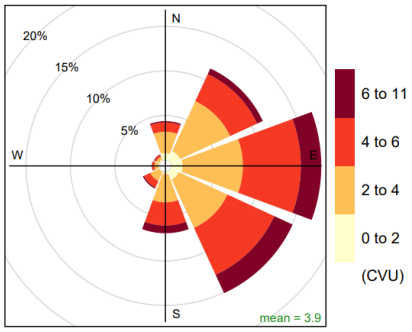

(b) Seasonal Frequency of Counts by Storm Direction (%)

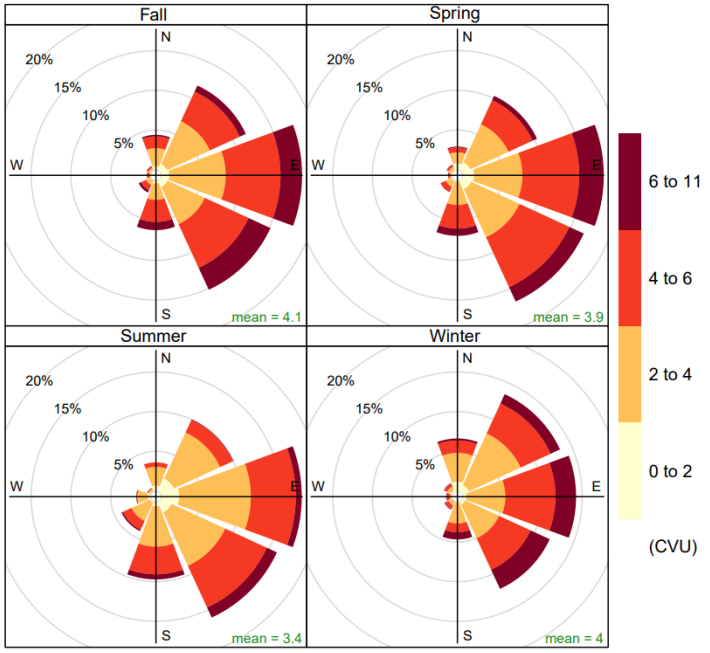

(c) Monthly Frequency of Counts by Storm Direction (%)

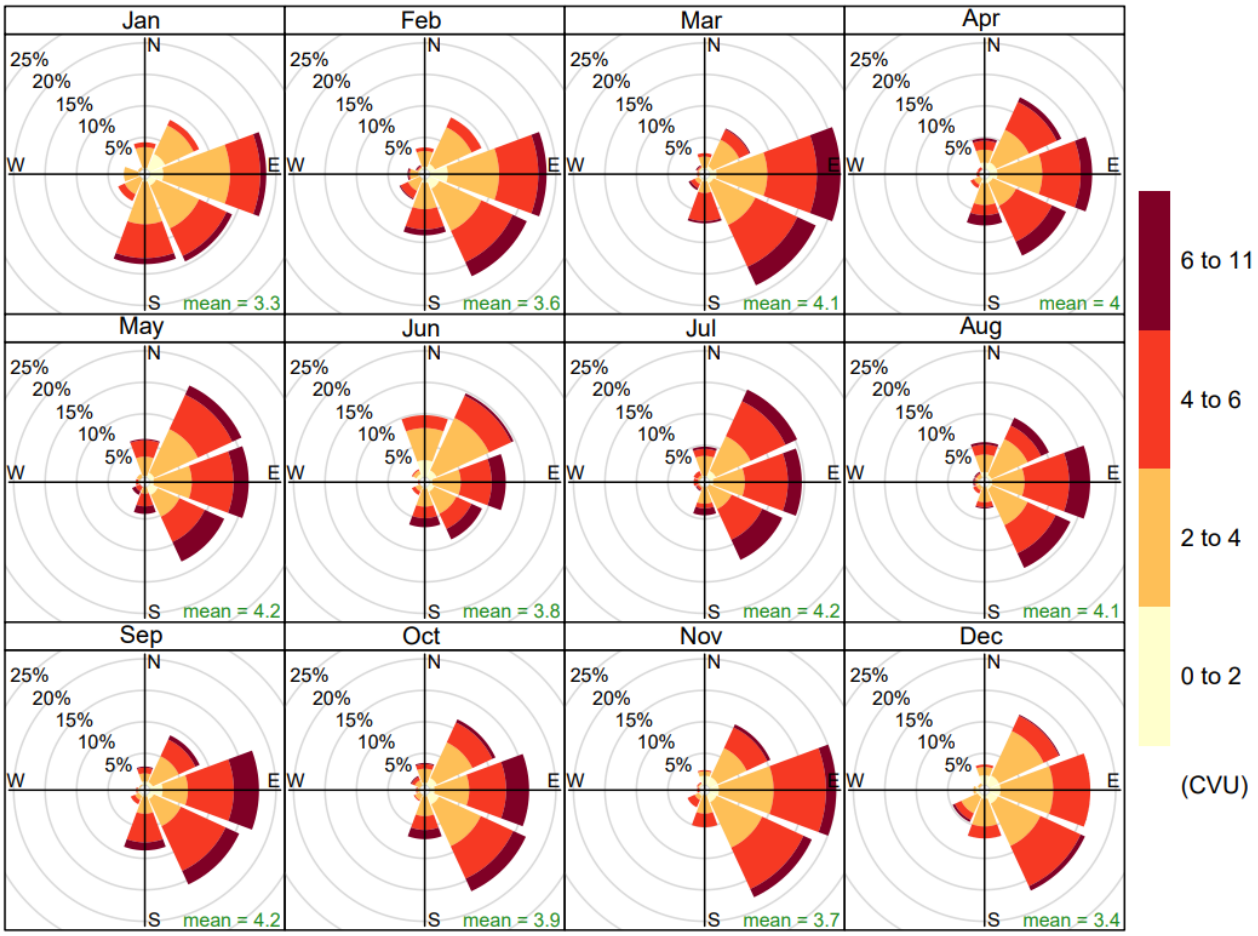

(d) Annual Frequency of Counts by Storm Direction (%)

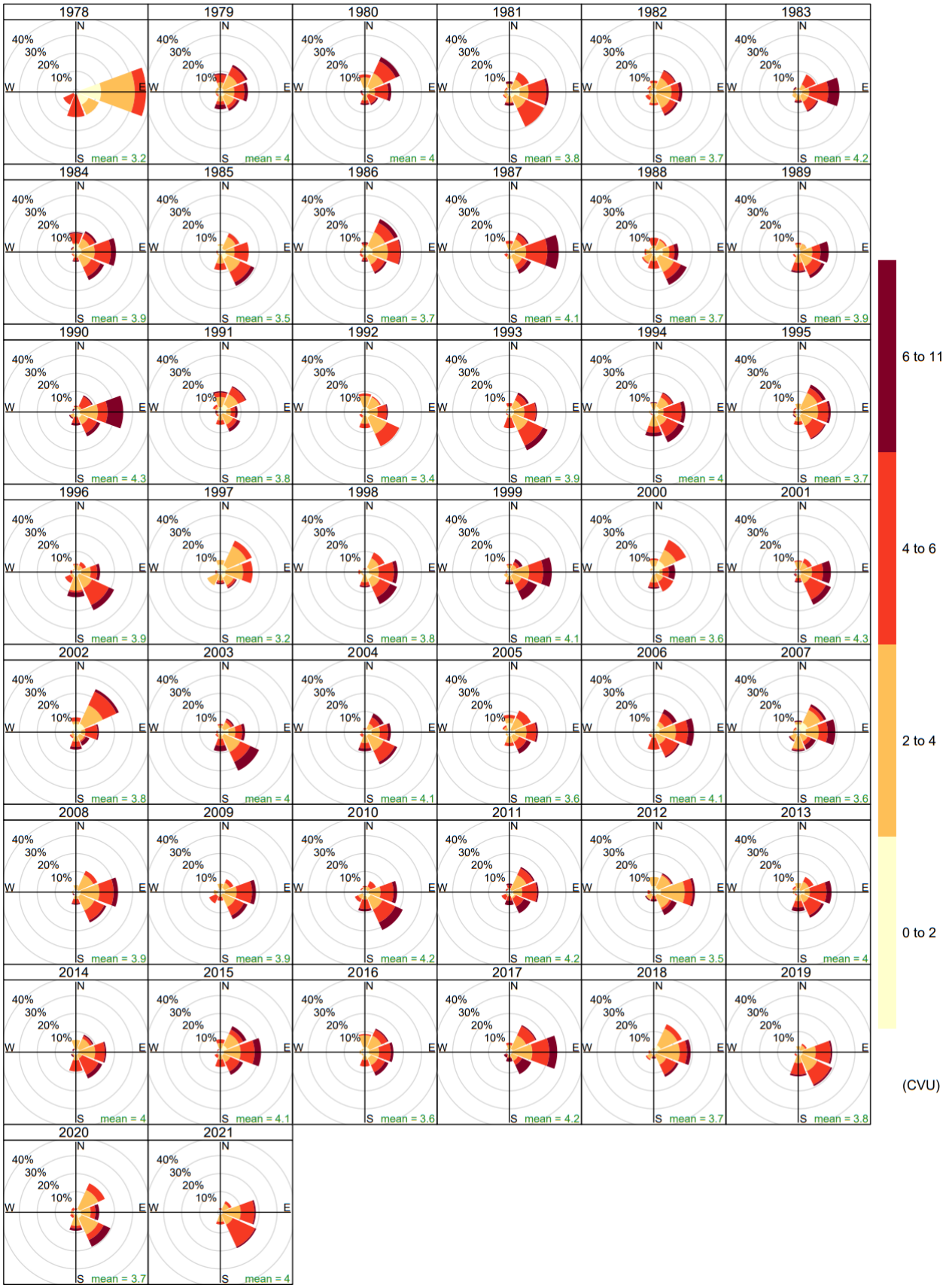

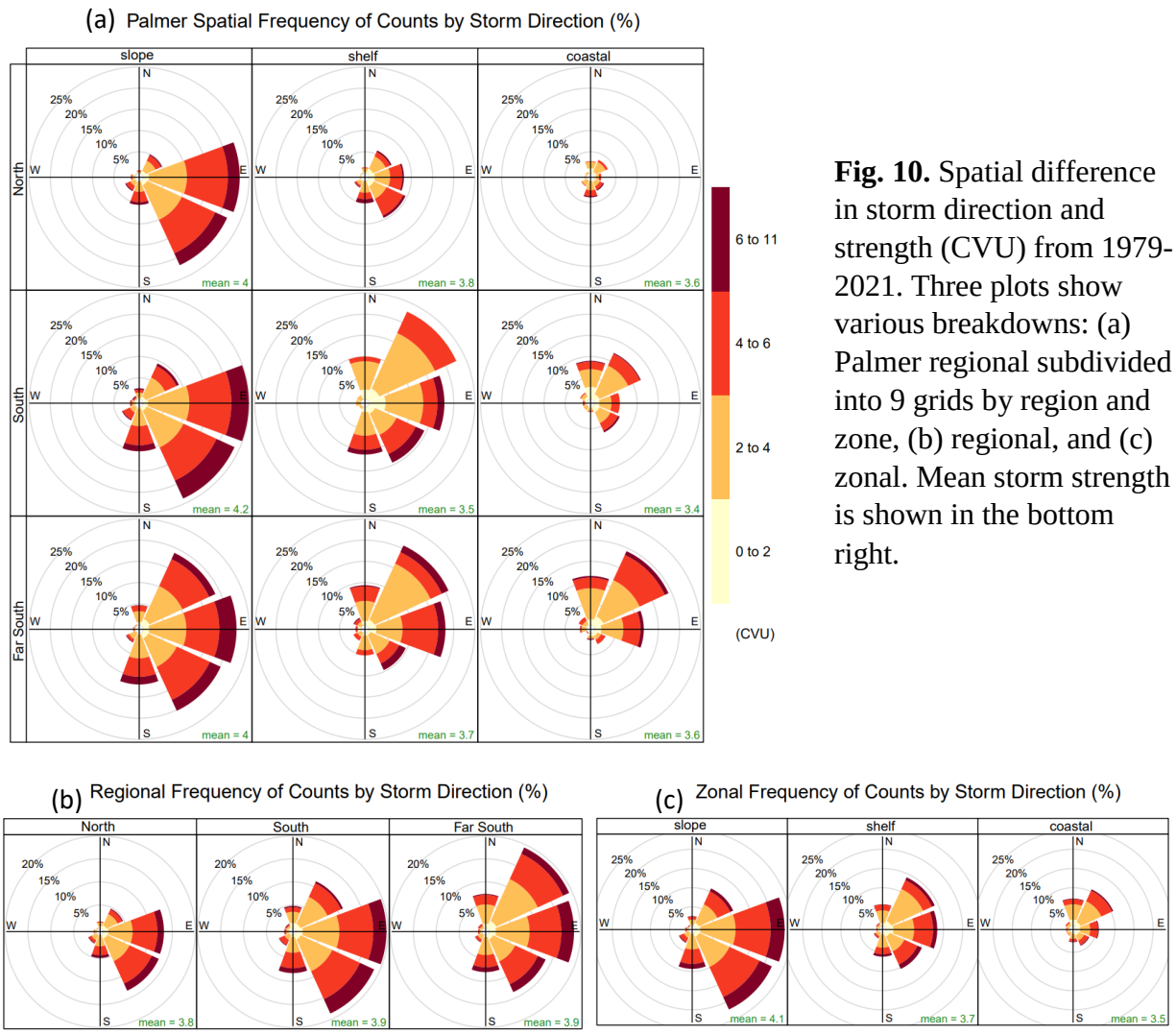

Fig. 10. Spatial difference in storm direction and strength (CVU) from 1979-2021. Three plots show various breakdowns: (a) Palmer regional subdivided into 9 grids by region and zone, (b) regional, and (c) zonal. Mean storm strength is shown in the bottom right.

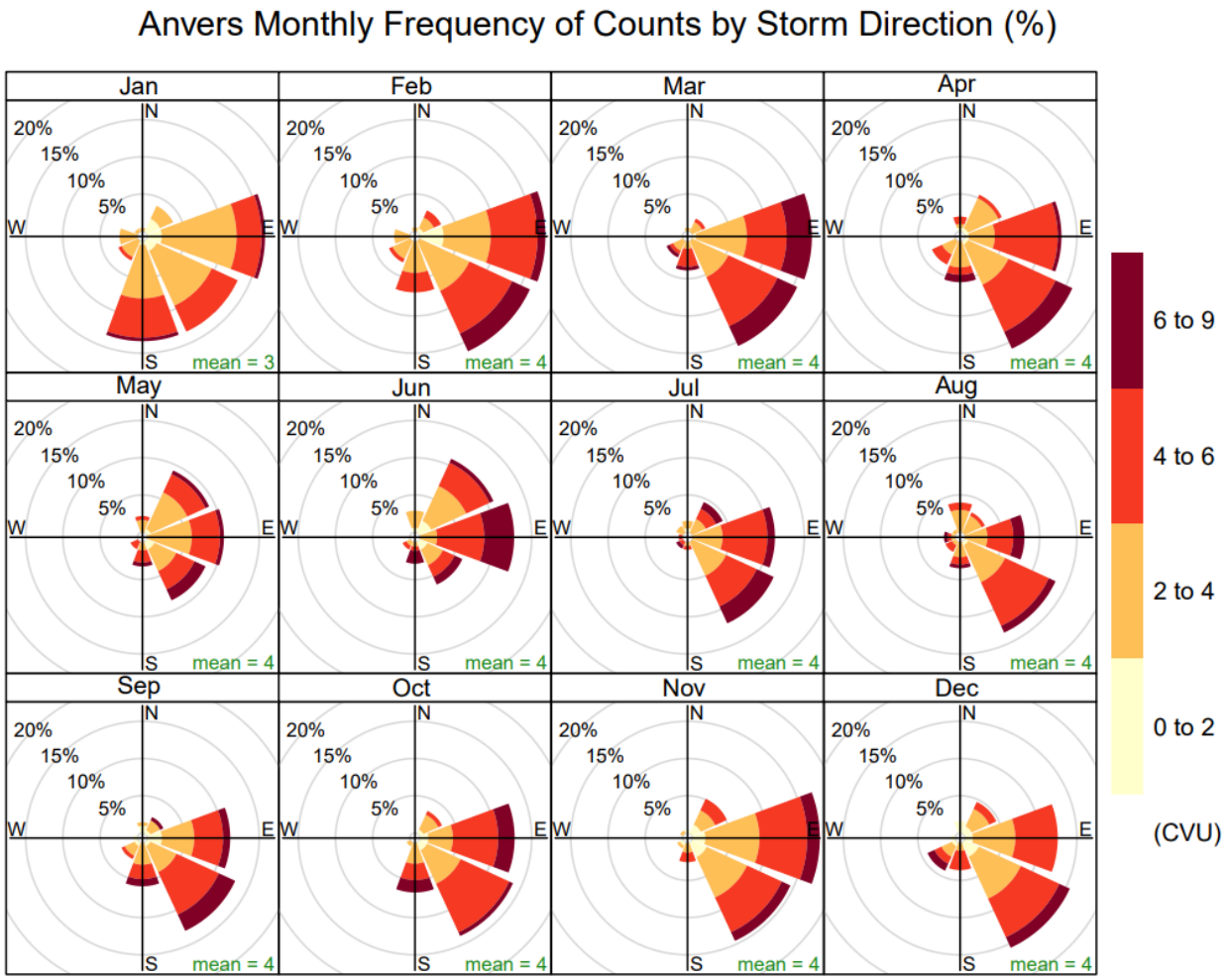

Fig. 11. Monthly frequency of counts by storm direction in the Northern region (Anvers) only from 1979-2021. Mean storm strength is shown in the bottom right.

Table 11. Comparison of mean storm characteristics via region. Test performed: group F-test with anova (F) for numeric variables, and a chi-squared test (X2) for non-numeric variables. N = number of observations, SD = standard deviation. Statistical significance shown via *p<0.1, **p<0.05, ***p<0.01.

Region	*North*			*South*			*Far South*			*Test*
Variable	*N*	*Mean*	*SD*	*N*	*Mean*	*SD*	*N*	*Mean*	*SD*	
Intensity	2381	3.8	1.5	1902	3.9	1.6	2029	3.9	1.5	F=3.234**
Zone	2381			1902			2029			X2=188.577**
Slyear	2381			1902			2029			X2=150.085***
Month	2381			1902			2029			X2=33.907*
Direction	962	121	57	1283	121	70	1433	107	74	F=18.655***
Duration	2381	1.5	0.84	1902	1.8	1.3	2029	1.6	1.2	F=38.511***

Table 12. Comparison of mean storm characteristics via zone. Test performed: group F-test with anova for numeric variables, and a chi-squared test for factor, logical, and character variables. Statistical significance shown via *p<0.1, **p<0.05, ***p<0.01.

Zone	*Slope*			*Shelf*			*Coast*			*Test*
Variable	*N*	*Mean*	*SD*	*N*	*Mean*	*SD*	*N*	*Mean*	*SD*	
Intensity	3510	4.1	1.6	1109	3.7	1.5	1693	3.5	1.5	F=77.047***
Region	3510			1109			1693			X2=188.577**
SIyear	3510			1109			1693			X2=159.025**
Month	3510			1109			1693			X2=48.794***
Season	3510			1109			1693			X2=32.712***
Direction	2537	119	58	587	109	77	554	106	98	F=9.802***
Duration	3510	1.9	1.3	1109	1.2	0.71	1693	1.3	0.63	213.464***

5.2 Sea Ice

Sea Ice Advance

Mean sea-ice advance for the entire PAL study area is year day 146 +/- 39 days (mean +/- SD) over the course of the study period. The mean day of year of sea-ice advance had a significant temporal trend for each of the three regions (north, south, and far south), all of which showed sea ice advancing later each year (Table 13). Sub-sites showed some statistical significant trends (Table S5, Fig 12). For the northern sites, only the coastal site had a $p<0.05$ and an upward trend. Southern sites had a positive temporal relationship with advance of sea ice at the coast and shelf sites. The Far Southern sites show significant positive slopes with each of the three sub-sites: coast, shelf, and slope.

Sea Ice Retreat

Mean sea-ice retreat is year day 342 +/- 40 days over the course of the study period (1979-2016). Sea ice retreat did not show any statistically significant temporal relationships. The mean retreat day trends at Far Southern coastal sites (Table S5, Fig. 13) were close to $p<0.05$.

Sea Ice Duration

Mean sea-ice duration is 197 +/- 70 days long over the course of the study period (1979-2016). The temporal trend in the mean duration of sea ice season exhibited a statistically significant negative trend for the combined sites for the North and the Far South region (Table

13). All sub sites in the Far South were significant as were South and North coastal sites (Table S5, Fig. 24).

Anvers Sea Ice: Penguin Foraging Site

Sea ice indices trends were investigated for the 200 km Adélie penguin foraging area for breeding colonies located near Anvers Island in the northern Palmer LTER study area. The day of sea-ice advance occurred later over time (0.7 day/year) for a total of 28.7 days later from 1979-2020 (Table 15, Fig. 15). Retreat of sea ice and duration of sea ice season did not exhibit a significant temporal change.

Sea Ice Index Interactions

Sea ice interactions near the Anvers penguin foraging area from 1979-2020 were investigated via linear regression to determine if timing of sea-ice advance may impact sea-ice retreat. A later advance correlated with an earlier retreat for all sub-sites in the South and for coastal sites in the North and Far South (Table 16).

Sea Ice Figures and Tables

Table 13. Mean sea ice indices and temporal trends for regions within Palmer Station study area 1979-2016. Units are in year-day for advance and retreat and in days for duration. Statistical significance shown via *p<0.1, **p<0.05, ***p<0.01. (n = 38)

Sea Ice Index	*Region*	*Mean*	*SD*	*Slope*	*R^2*	*P-value*	*Significance*
Advance	**North**	**150**	**32.1**	**0.9804**	**0.1647**	**0.0115**	**
	South	**151**	**25.9**	**0.8084**	**0.1435**	**0.019**	**
	Far South	**117**	**37.7**	**1.3852**	**0.2804**	**0.000629**	***
Retreat	North	327	42.8	-0.442	0.02486	0.3444	*
	South	336	34.7	-0.2899	0.0129	0.4972	*
	Far South	363	33.6	-0.6809	0.09135	0.0651	*
Duration	**North**	**159**	**63.4**	**-1.4244**	**0.1082**	**0.04379**	**
	South	187	52.2	-1.1011	0.07591	0.09408	*
	Far South	**247**	**61.8**	**-2.0673**	**0.2605**	**0.00106**	***

Table 14. Mean sea ice indices and temporal trends for zones within Palmer Station study area 1979-2016. Units are in year-day for advance and retreat and in days for duration. Statistical significance shown via *p<0.1, **p<0.05, ***p<0.01. (n = 38)

Sea Ice Index	*Region*	*Slope*	*SE*	*R^2*	*P-value*	*Significance*
Advance	**coastal**	**1.62**	**0.364**	**0.151**	**0.0000193**	***
	shelf	**0.996**	**0.289**	**0.0959**	**0.000799**	***
	slope	**0.554**	**0.223**	**0.0524**	**0.0143**	**
Retreat	**coastal**	**-0.612**	**0.264**	**0.0458**	**0.0222**	**
	shelf	-0.442	0.306	0.0183	0.151	
	slope	-0.359	0.311	0.0117	0.251	
Duration	**coastal**	**-2.24**	**0.547**	**0.13**	**0.0000804**	***
	shelf	**-1.44**	**0.519**	**0.0647**	**0.0063**	***
	slope	**-0.909**	**0.453**	**0.0347**	**0.0473**	**

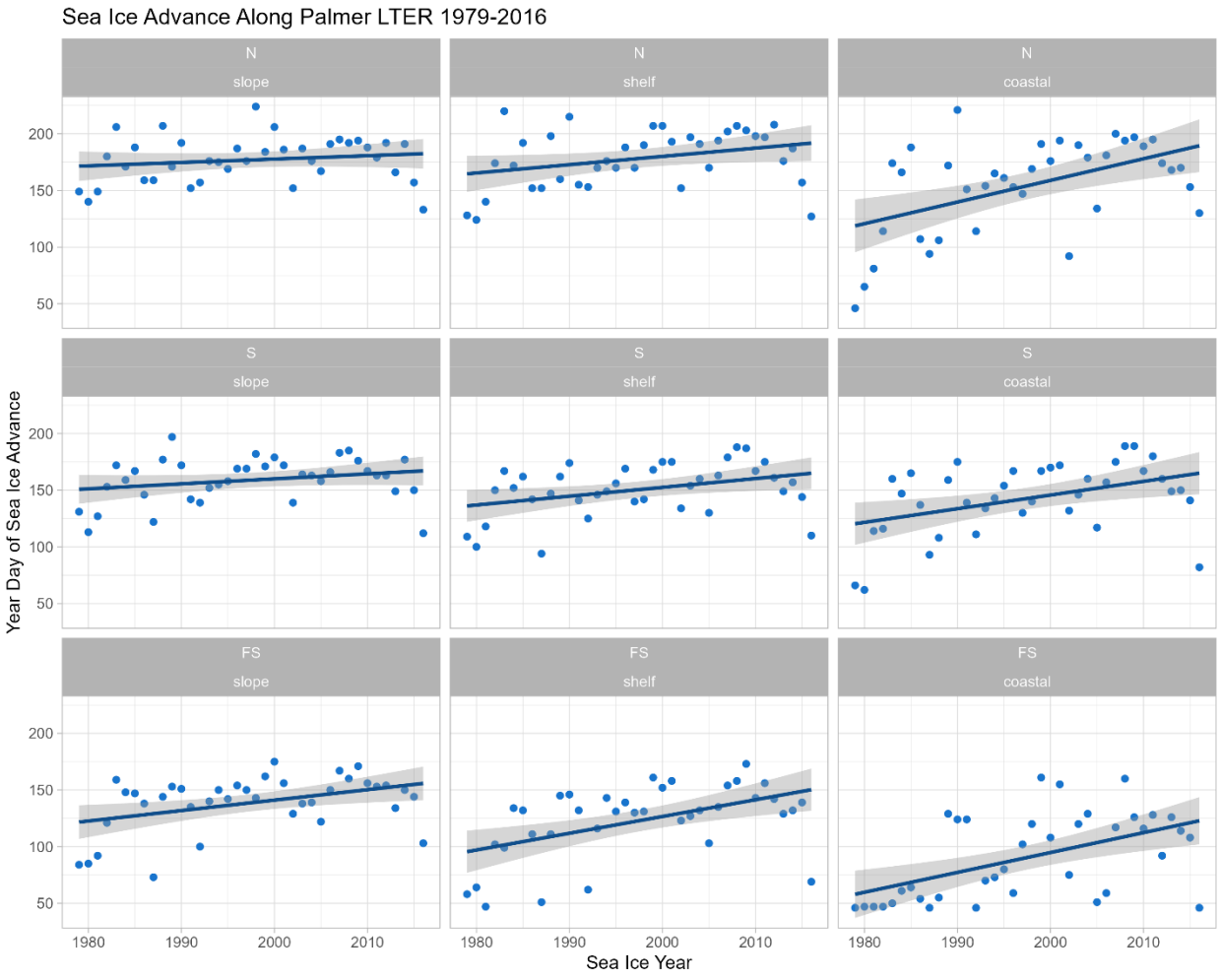

Fig 12. Day of sea-ice advance in Palmer Station study area divided into region (north, south, far south) and zone (coast, shelf, slope) sub-sites from 1979-2016. The line represents estimated slope with 95% confidence intervals shown in gray.

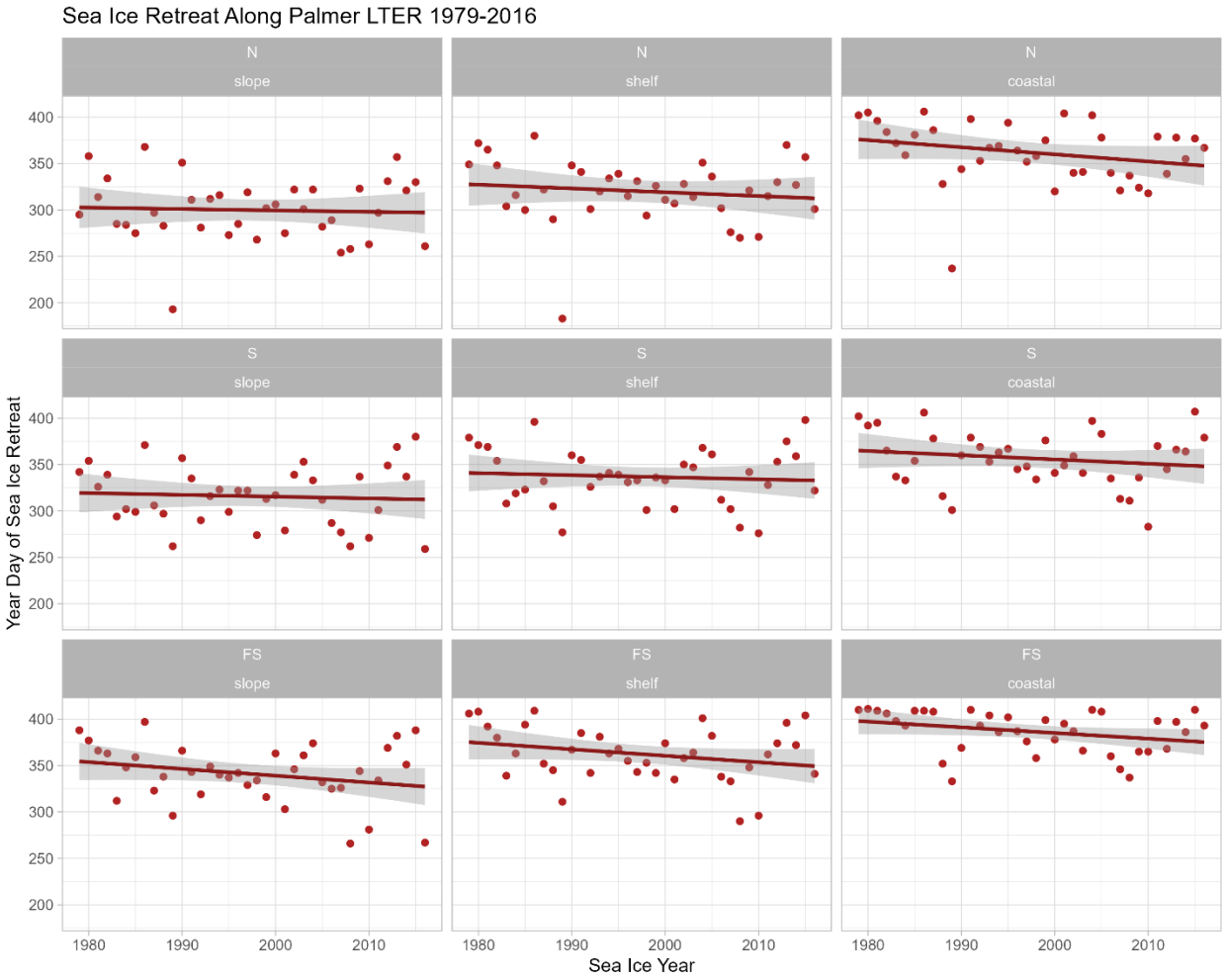

Fig 13. Sea ice retreat in Palmer Station study area divided into region (north, south, far south) and zone (coast, shelf, slope) sub-sites from 1979-2016. The line represents estimated slope with 95% confidence intervals shown in gray.

Fig 14. Sea ice duration in Palmer Station study area divided into region (north, south, far south) and zone (coast, shelf, slope) sub-sites from 1979-2016. The line represents estimated slope with 95% confidence intervals shown in gray.

Table 15. Sea ice indices for Anvers Region 1979-2020. Units are in year-day for advance and retreat and in days for duration. (n=42).

Sea Ice Index	*Mean*	*SD*	*Slope*	*SE*	*R^2*	*P-value*	*Significance*
Advance	**175**	**25**	**0.6978**	**0.3049**	**0.09367**	**0.02746**	**
Retreat	322	34	-0.1775	0.4415	-0.02088	0.6899	
Duration	148	45	-0.8768	0.5619	0.03382	0.1265	

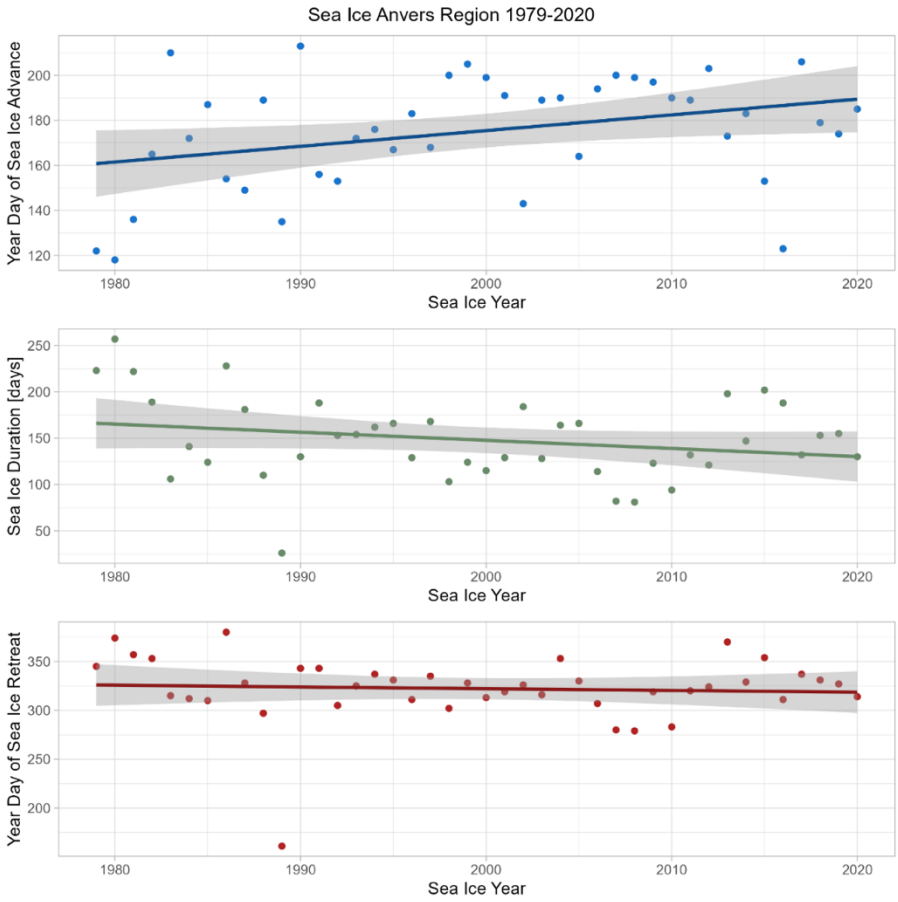

Fig 15. Sea ice advance, duration, and retreat at Anvers penguin foraging area from 1979-2020. Line represents linear trend and gray area represents 95% confidence intervals.

Table 16. Correlation between day of sea-ice retreat and day of sea-ice advance for each sub-site in the Palmer Station study area (1979-2016). Regions: N = north, S = south, FS = far south. Units are day of yr/day of yr.

Region	Zone	Slope	SE	R2	P-Value	Significance
FS	**coastal**	**-0.248**	**0.0917**	**0.169**	**0.01**	*
FS	**shelf**	**-0.296**	**0.141**	**0.109**	**0.04**	**
FS	slope	-0.233	0.208	0.0335	0.27	
S	**coastal**	**-0.469**	**0.135**	**0.251**	**0.001**	***
S	**shelf**	**-0.526**	**0.2**	**0.161**	**0.012**	**
S	**slope**	**-0.506**	**0.255**	**0.0985**	**0.0549**	*
N	**coastal**	**-0.306**	**0.125**	**0.142**	**0.0198**	**
N	**shelf**	**-0.417**	**0.22**	**0.0904**	**0.0666**	*
N	slope	-0.359	0.276	0.045	0.201	

5.3 Snow

Snow measurements are from Palmer Station. Since there is no spatial component, snow depth provides constraints on temporal changes and variability. There is a fair amount of inter-annual variability in mean snow depth (Fig 16). Each seasons' snow depth is significantly different from each other ($p<0.001$, Fig 27) and most months are significantly different except for: Nov-Aug, Mar-Jan, Dec-May, Mar-Feb, Feb-Jan (Table S6). Winter and fall snow depths are decreasing, whereas summer and spring snow depths are increasing (Table 17).

Table 17. Seasonal differences in snow depths. Statistical significance shown via *p<0.1, **p<0.05, ***p<0.01. Mean units are cm and slope units are cm/yr.

Season	*Mean*	*Stdev*	*Slope*	*SE*	*R2*	*P-value*	*Signif*
Winter	43.0	18.5	-0.1	0.04	0.002	0.007	***
Spring	62.0	32.6	0.7	0.08	0.316	0.000	***
Summer	7.4	22.3	0.4	0.05	0.027	0.000	***
Fall	11.0	13.9	-0.3	0.03	0.401	0.000	***

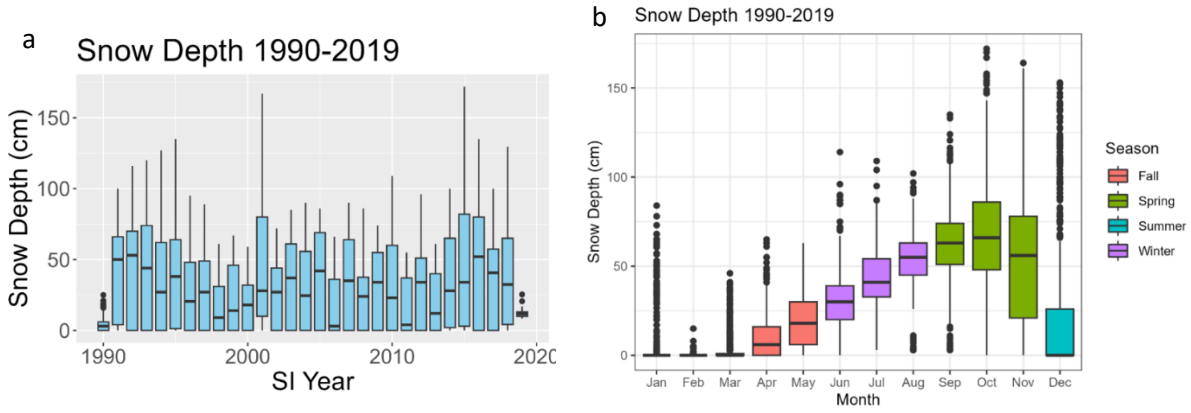

Fig 16. Daily snow depth (cm) from Palmer Station 1990-2019. (a) Snow depth annual variability at Palmer Station (incomplete sampling in 1990 and 2019). (b) Variability of snow depth for each month and season.

5.4 Interactions Among Storms, Sea Ice, and Snow

While there were no significant correlations between storm frequency and sea-ice advance, annual storm frequency positively correlates with sea-ice retreat for the entire coastal region, and in the sub-sites North coastal, and Far South coastal (Table 18, Fig. 17). This finding was opposite of the original hypothesis. Mean storm intensities for all storms were tested using linear regression with sea ice indices. Results showed a few cases of statistically significant

relationships (Table 19). The regional overall exhibited a later advance when storm intensity increases. Both the North and Far South coastal sites had significant correlation with all season mean storm intensity and day of advance (Fig 18). There were no significant findings between duration or direction of storm and sea ice indices. Advance and winter bearing were close to being significant (p=0.058) where direction shifts 1 unit of degree (i.e. more southern winds) correlates with the day of advance occurring later by 0.17 +/- 0.09 days. Seasonal storm characteristics were used as predictor variables for sea ice indices. AIC was used to determine the best fitting model. A linear model was used to predict sea-ice advance (Table 20), sea-ice retreat (Table 21), and sea-ice duration (Table 22). A linear model was used to predict November snow depth from spring storm characteristics which showed that storm frequency is positively correlated with snow depth. (Table 23). November snow depth is of interest because it is a known factor that influences mean clutch initiation date (Cimino et al. 2019).

Physical Interactions Figures and Tables

Table 18. Correlation results from linear regression between day of retreat (dependent variable) and storm frequency (independent variable) within all of the Palmer Station study region. Slope is day of year / number of storms. Statistical significance shown via *p<0.1, **p<0.05, ***p<0.01.

Region	*Zone*	*Slope*	*SE*	*R2*	*P-value*	*Signif*
All	*Coastal*	0.9945	0.3227	0.111075	0.0028668	***
North	*Coastal*	1.482	0.4711	0.2919	0.00438	***
Far South	*Coastal*	0.8014	0.4169	0.1334	0.066499	*

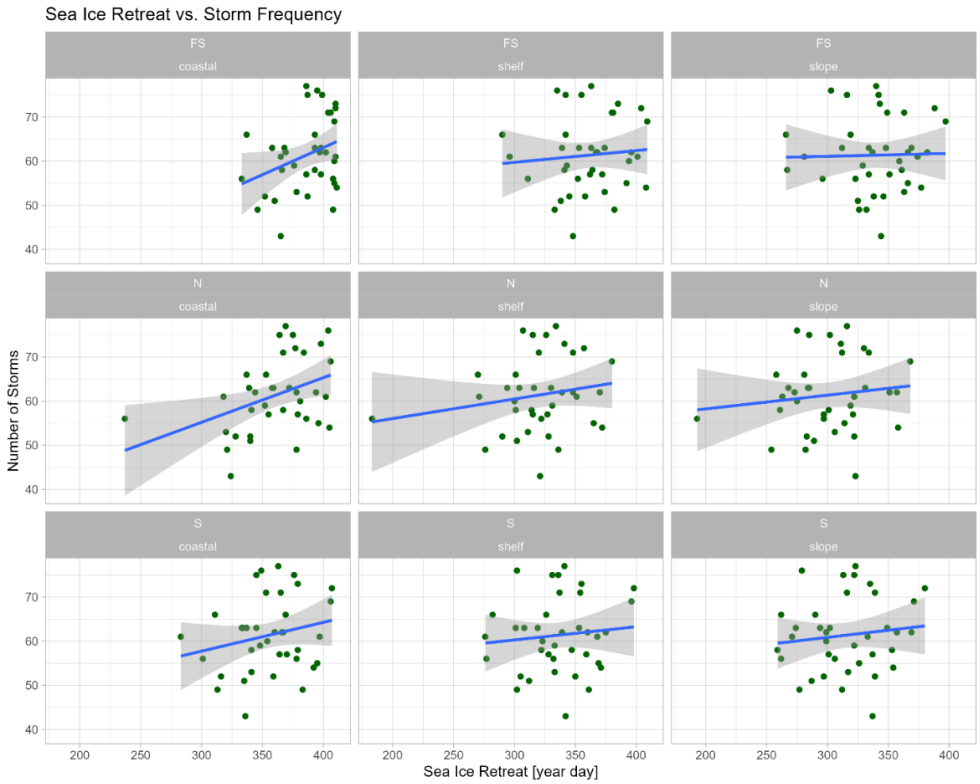

Fig 17. Linear regression between storm frequency within the Palmer Station study area and sea-ice retreat for each sub-site (region-zone). N = North, S= South, FS = Far South.

Table 19. Significant correlation results from linear regression between day of advance (dependent variable) and storm intensity (independent variable) within all of the Palmer Station study region. Slope is day of year / CVU. Statistical significance shown via *p<0.1, **p<0.05, ***p<0.01.

Region	Zone	Slope	SE	R^2	P-Value	Signif
All	**coastal**	**50.8**	**16.0**	**0.118**	**0.00211**	***
All	**shelf**	**32.7**	**12.2**	**0.0869**	**0.00881**	***
All	slope	13.3	9.5	0.0249	0.168	
FS	**All**	**41.1**	**12.9**	**0.118**	**0.00211**	***
S	**All**	**27.2**	**8.3**	**0.123**	**0.00161**	***
N	**All**	**28.5**	**9.6**	**0.105**	**0.00383**	***
FS	**coastal**	**59.7**	**23.0**	**0.219**	**0.0158**	**
FS	**shelf**	**44.1**	**16.7**	**0.225**	**0.0143**	**
FS	slope	19.6	12.9	0.087	0.143	
S	**coastal**	**41.6**	**16.5**	**0.209**	**0.0188**	**
S	**shelf**	**30.0**	**13.3**	**0.176**	**0.0328**	**
S	slope	9.9	12.3	0.0265	0.427	
N	**coastal**	**51.2**	**17.6**	**0.261**	**0.00765**	***
N	shelf	24.1	15.3	0.0942	0.127	
N	slope	10.2	14.3	0.0211	0.479	

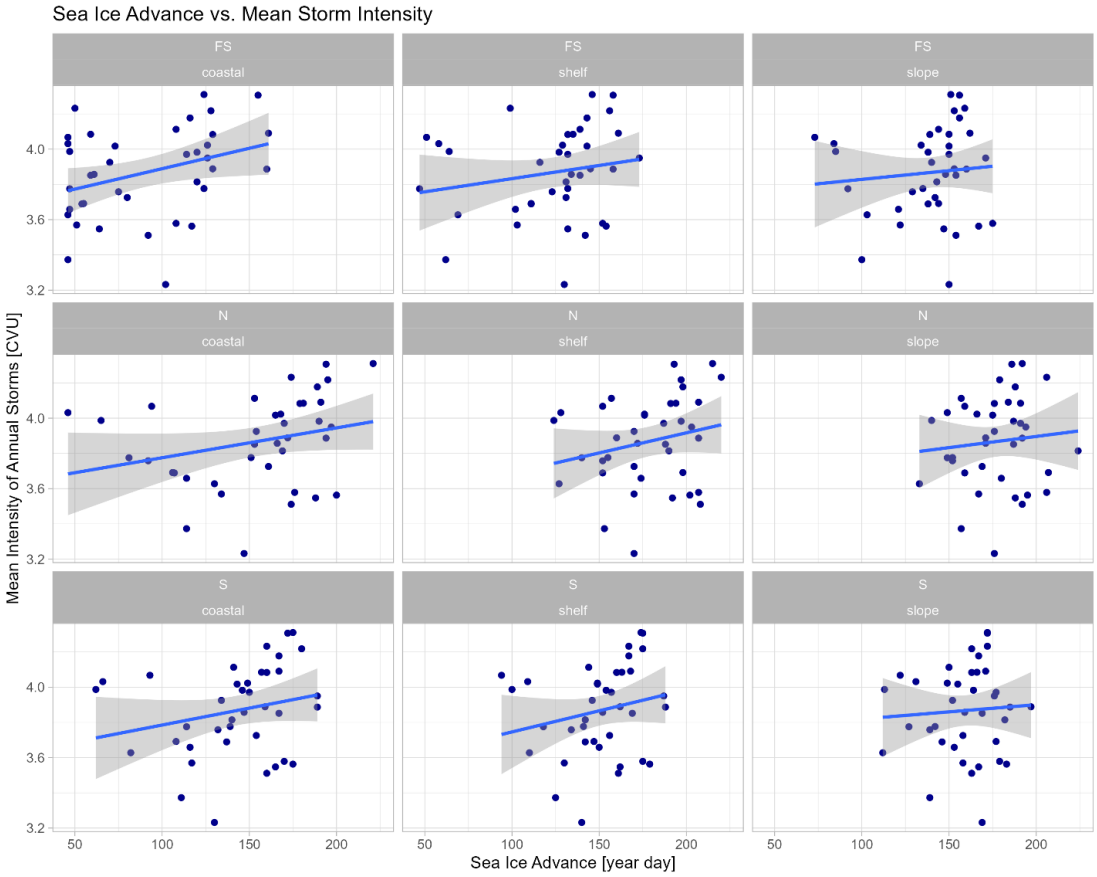

Fig 18. Linear regression between storm intensity within the Palmer Station study area and sea-ice advance for each sub-site (region-zone). N = North, S= South, FS = Far South.

Table 20. Linear model for day of sea-ice advance predicted by storm characteristics (formula: advance ~ $intensity_{win}$ + $intensity_{spr}$+ $intensity_{sumr}$ + $duration_{win}$ + $duration_{sumr}$ + $direction_{win}$ + $frequency_{win}$ + $frequency_{sumr}$). Adjusted R^2 = 0.1918, explains 19% of the variation in sea-ice advance. Statistical significance shown via *p<0.1, **p<0.05, ***p<0.01.

Variable	Season	Slope	StdError	P-Value	Signif
Intensity	**Winter**	**21.2**	**4.9393**	**0.00002**	***
Intensity	**Spring**	**18.14**	**3.7363**	**0.00000**	***
Intensity	**Summer**	**-18.39**	**6.1204**	**0.00296**	***
Duration	**Winter**	**-20.14**	**10.011**	**0.04544**	**
Duration	Summer	5.13	3.1590	0.10587	
Direction	Winter	0.21	0.1151	0.06886	*
Frequency	**Winter**	**-1.32**	**0.4886**	**0.00725**	***
Frequency	**Summer**	**0.92**	**0.4646**	**0.04908**	**

Table 21. Linear model for day of sea-ice retreat predicted by storm characteristics (formula: retreat ~ $intensity_{spr}$ + $intensity_{sumr}$ + $intensity_{fall}$ + $duration_{fall}$ + $direction_{spr}$ + $direction_{sum}$ + $direction_{fall}$ + $frequency_{win}$ + $frequency_{spr}$). Adjusted r^2 = 0.1845, explains 18% of the variance in sea-ice retreat. Statistical significance shown via *p<0.1, **p<0.05, ***p<0.01.

Variable	Season	Slope	StdError	P-Value	Signif
Intensity	Spring	9.2363	4.7183	0.051527	*
Intensity	**Summer**	**22.6438**	**6.8452**	**0.001095**	***
Intensity	**Fall**	**-28.0879**	**6.5750**	**0.000028**	***
Duration	**Fall**	**-21.1827**	**6.8150**	**0.002126**	***
Direction	Spring	-0.2113	0.1384	0.128212	
Direction	**Summer**	**-0.4261**	**0.1199**	**0.000463**	***
Direction	**Summer**	**0.3157**	**0.1572**	**0.045775**	**
Frequency	**Winter**	**2.3094**	**0.6532**	**0.000495**	***
Frequency	Summer	-1.4720	0.6434	0.023086	**

Table 22. Linear model for sea-ice duration predicted by storm characteristics (formula: duration ~ $intensity_{winter}$ + $intensity_{spring}$ + $intensity_{sumr}$ + $intensity_{fall}$ + $duration_{summer}$ + $duration_{fall}$ + $frequency_{win}$ + SIyear). Adjusted r^2 = 0.1599, explains almost 16% of the variance in sea-ice duration. Statistical significance shown via *p<0.1, **p<0.05, ***p<0.01.

Variable	Season	Slope	StdError	P-Value	Signif
Intensity	**Winter**	**-35.8552**	**8.9473**	**0.000084**	***
Intensity	**Spring**	**-19.7334**	**7.3142**	**0.007505**	***
Intensity	**Summer**	**46.3441**	**11.337**	**0.000060**	***
Intensity	**Fall**	**-38.5332**	**10.8460**	**0.000464**	***
Duration	**Summer**	**-13.0545**	**6.3075**	**0.039623**	**
Duration	**Fall**	**-26.3453**	**10.6805**	**0.014384**	**
Frequency	**Winter**	**3.3399**	**1.0524**	**0.001715**	***
SI year	**n/a**	**1.8301**	**0.6045**	**0.002754**	***

Table 23. Linear model for November snow depth predicted by spring storm characteristics (snow depth ~ $intensity_{spring}$ + $duration_{spring}$ + $frequency_{spring}$ + SIyear). Adjusted R2 =0.02657, explains about 2.7% of the variance. Slope = cm/unit of change. Statistical significance shown via *p<0.1, **p<0.05, ***p<0.01.

Variable	Slope	SE	P-Value	Signif
Intensity	-0.109	0.70832	0.8777	
Duration	0.748	1.03605	0.4706	
Frequency	**1.070**	**0.08154**	**0.0000**	***
SI year	0.085	0.04682	0.0679	*

5.5 Impacts on Adélie Penguin

Adélie CFM

Adélie penguin chick fledging mass (CFM) data are normally distributed (Fig. S11) and show within season variability as well as inter-annual variability with an overall average mass of 3063.8 g (stdev = 357, n=6373) (Fig19). Results do not show a linear trend for mean fledging mass over time ($p>0.05$) (Fig 20, Fig. S13). When all chick mass data are utilized, a temporal trend appears to have a slight uptick in weights (slope=1.1416, error estimate = 0.5955, $p=0.0553$, $R^2=0.0005765$; Figure S12).

The influence of storms on penguin metrics is evaluated in two different model suites: 1) annual averages of storms and annual average CFM, and 2) seasonal averages of storms and average CFM. Predictor variables were investigated in their individual correlation with the response variable, CFM. Linear models show a significant negative correlation between CFM and frequency, intensity, and direction of storms (Fig. 21, Table 24). Most notably, 1-unit of intensity increase results in a CFM loss of nearly 46 grams.

The influence of storms on CFM is evaluated in model suite 1) annual averages of storms and annual averages of CFM. Before running models, predictor variables are checked for collinearity (Fig. 22). No significant correlations were found and distribution of data appears normal (with the exception of average duration). A linear model (LM1) was run with all variables ($CFM_{avg} \sim intensity_{avg} + direction_{avg} + duration_{avg} + frequency_{yr}$ + SI year) with no significant ($p<0.05$) variables found (Table 25). Residuals appear normal (Fig. S14) and no autocorrelation structure was found via ACF and PACF (Fig. S15). However, R^2 was low and variance explained is only 1.05%. Next a linear mixed model was run via the glmmTMB package under a Gaussian distribution ($CFM_{avg} \sim intensity_{avg} + direction_{avg} + duration_{avg} + frequency_{yr}$ + SI year). Results of the multiple regression model showed a significant relationship ($p<0.05$) between chick mass and annual frequency of storms, and when storm count is increased by 1, chick mass decreases by 1.4 grams (Table 26). Validity of the model was approved via the DHARMa package which compares model residuals with the observed (Fig. 23).

The influence of storms on CFM is evaluated in model suite 2) seasonal averages of storms and average CFM. Prior to running models, variables are checked for collinearity (Fig S16). No significant correlations were found. Residuals appear normal (Fig. S17) and no

concerning autocorrelation structure was found via ACF and PACF (Fig. S18). Next a linear mixed model (LMM) was run with all environmental variables and SI year a random effect. Results of LMM showed a significant relationship ($p<0.05$) between CFM and spring storm intensity, duration of summer storms, direction of spring and fall storms, and the frequency of spring and summer storms (Table 28). The intensity of spring storms and duration of summer storms had the greatest negative influence on CFM, lowering mass by 57g and 71g respectively. Validity of the model was checked via the DHARMa package which compares model residuals with the observed (Fig. 24). The model passed the KS and dispersion tests, however it failed the outliers test.

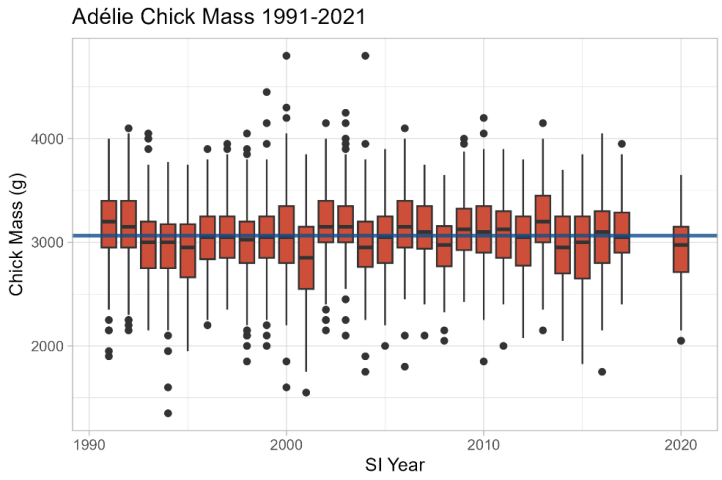

Fig 19. Adélie chick fledging mass from 1991-2021 from Humble Island. The blue line represents the mean (3064 g ± 357 SD, n=6373).

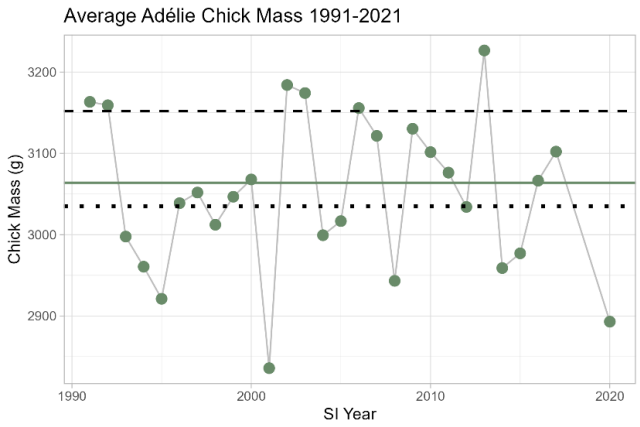

Figure 20. Average chick fledging mass over time (1991-2021). Dotted lines represent mean non-survivor mass (CFM < 3.035 kg) and dashed represents survivor mass (CFM > 3.152 kg).

Green line represents mean CFM over study period (mean = 3064 g, stdev =357, n=6373). No significant trend over time (slope=-1.052, p=0.6139, R^2 = 0.009559).

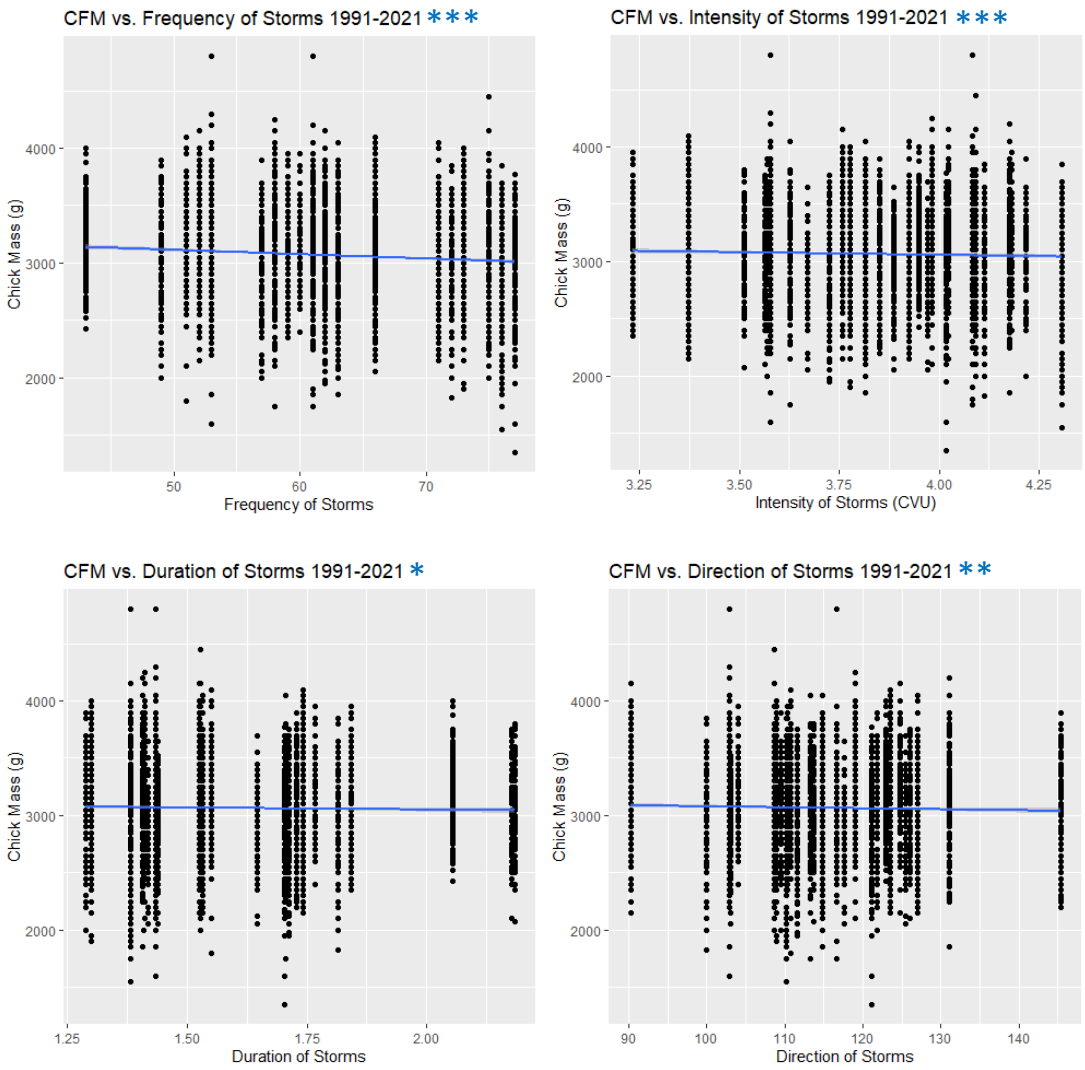

Fig 21. Linear model of annual averaged storm characteristics vs. chick fledging mass. Linear trends significant for frequency, intensity, and direction of storms with CFM (Table 25). Statistical significance shown via *p<0.1, **p<0.05, ***p<0.01.

Table 24. Model output for linear regression of annual average storm characteristics vs. chick fledging mass. Statistical significance shown via *p<0.1, **p<0.05, ***p<0.01.

Model	*Slope (g/unit)*	*SE*	*T-value*	*R^2*	*P-value*	*Signif*
mass ~ freq	-3.7754	0.4823	-7.828	0.00937	5.78e-15	***
mass ~ int	-45.63	17.05	-2.676	0.0009658	0.007473	***
mass ~ dur	-34.60	20.16	-1.716	0.0003052	0.08618	*
mass ~ dir	-0.8592	0.3757	-2.287	0.0006635	0.02223	**
mass ~ SIyear	1.1416	0.5955	1.917	0.0004197	0.05527	*

Table 25. LM1 Model results (CFM_{avg} ~ int_{avg} + dir_{avg} + dur_{avg} + $freq_{yr}$ + SI year). R^2 = 0.01056. Statistical significance shown via *p<0.1, **p<0.05, ***p<0.01.

Variable (Annual)	*Estimate (g/unit)*	*StdError*	*P-value*	*Signif*
Intensity (avg)	-15.4	73.7	0.836	
Bearing (avg)	0.383	1.68	0.822	
Duration (avg)	38.3	81.2	0.642	
Frequency	0.754	0.754	0.0732	*

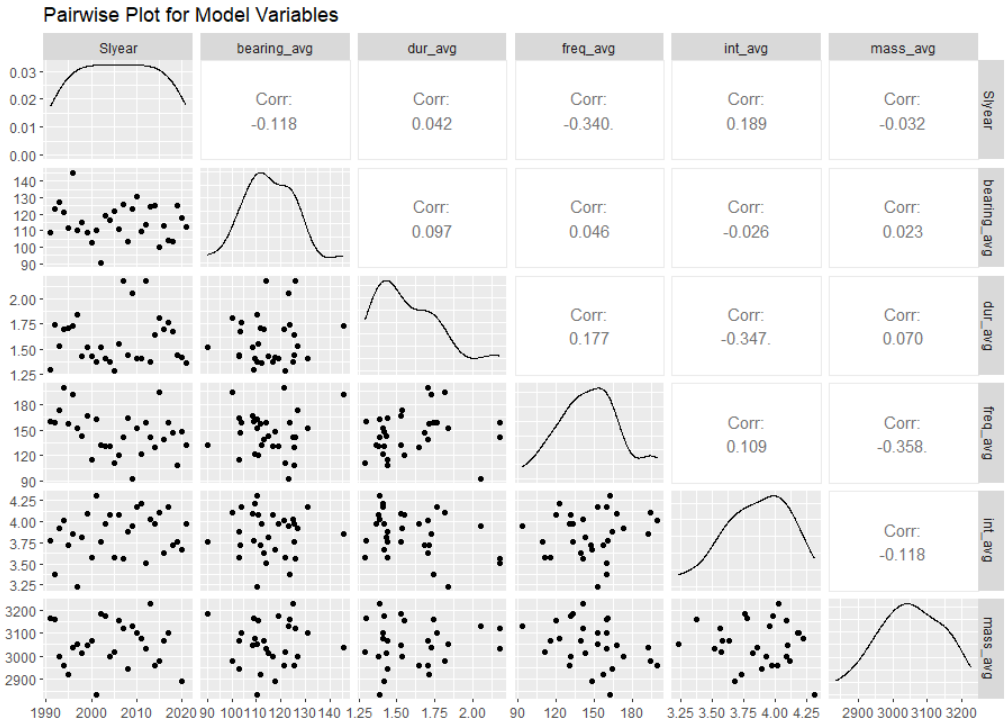

Fig. 22. Pairwise plot for model variables. No significant (p<0.05) correlations were found. Shown here are scatterplots of the data (bottom left panels), distribution of data (diagonal middle panels), and correlation coefficients between each variable (top right panels).

Table 26. Linear Mixed Model results (formula: CFM_{avg} ~ $intensity_{avg}$ + $direction_{avg}$ + $duration_{avg}$ + $frequency_{yr}$ + SI year). Conditional R2: 0.061, weak model only explaining 6.1%. Statistical significance shown via *p<0.1, **p<0.05, ***p<0.01.

Variable (Annual)	*Estimate (g/unit)*	*SE*	*P-value*	*Signif*
Intensity (avg)	-15.4149	66.7613	0.8174	
Bearing (avg)	0.3836	1.5228	0.8016	
Duration (avg)	38.2514	73.6186	0.6033	
Frequency	-1.4155	0.6833	0.0383	**

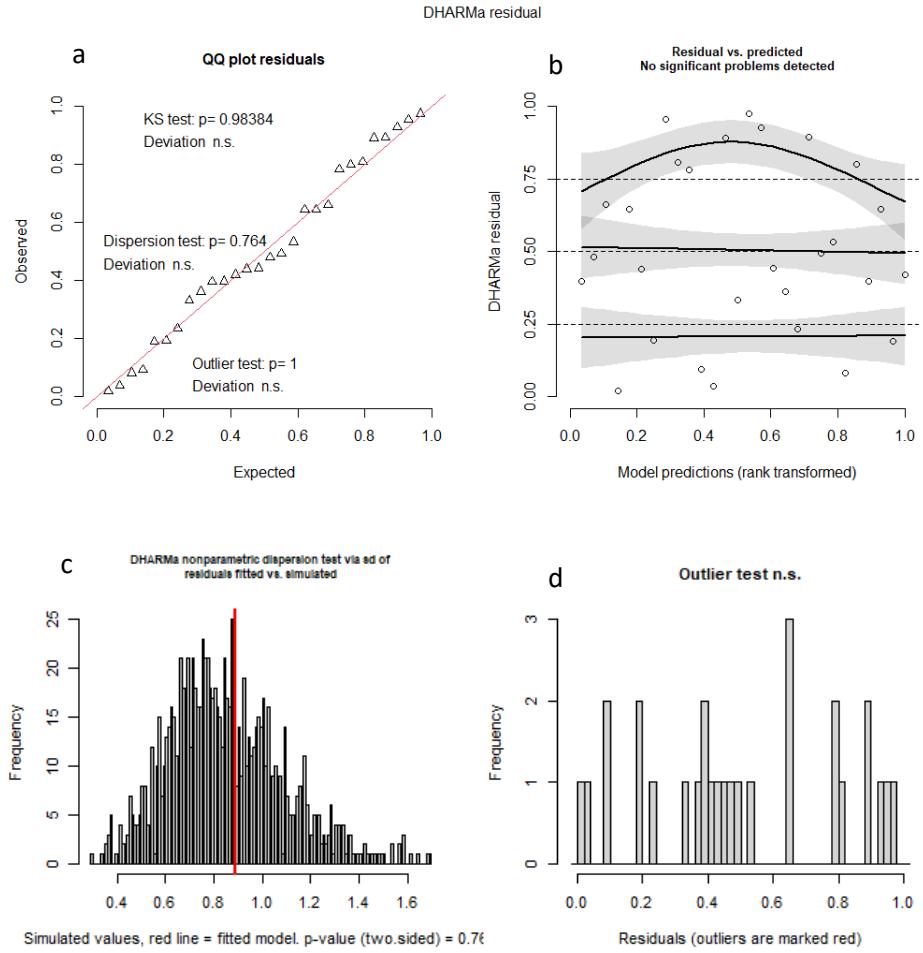

Figure 23. DHARMa model validation for LMM for annual averages of storm characteristics as a predictor of average CFM. (a) QQ plot residuals of expected vs. observed. (b) residuals vs. predicted. (c) distribution of residuals. (d) outlier test. Results from these test indiciate a good model fit.

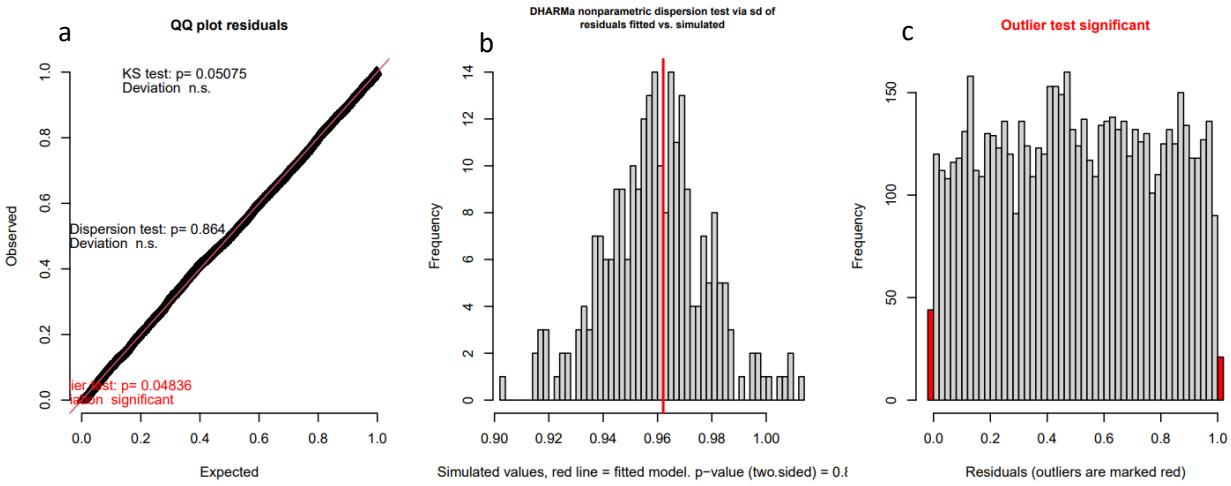

Figure 24. Seasonal LMM predicting mean CFM from seasonally averaged storm characteristics. (a) QQ plot residuals of expected vs. observed. (c) distribution of residuals. (c) outlier test. Results from these test indiciate a good model fit.

Table 27. Seasonal linear mixed model results (CFM_{avg} ~ $intensity_{sum}$ + $intensity_{fall}$ + $intensity_{spring}$ + $duration_{sum}$ + $duration_{win}$ + $duration_{spring}$+ $direction_{sum}$ + $direction_{fall}$ + $direction_{win}$ + $direction_{spring}$ + $frequency_{sum}$ + $frequency_{fall}$ + $frequency_{win}$ + $frequency_{spring}$ + (1 | SI year). R2=0.061. Statistical significance shown via *p<0.1, **p<0.05, ***p<0.01.

Variable (Average)	*Season*	*Estimate (g/unit)*	*SE*	*P-value*	*Signif*
Intensity	**Spring**	**-57.05**	**25.8455**	**0.02728**	**
Intensity	**Summer**	**77.80**	**39.5150**	**0.04896**	**
Intensity	Fall	-3.34	33.9463	0.92164	
Duration	Winter	-39.49	62.6375	0.52838	
Duration	Spring	-18.19	41.5137	0.66134	
Duration	**Summer**	**-70.72**	**24.8254**	**0.00439**	***
Direction	Winter	-0.71	0.7010	0.30918	
Direction	**Spring**	**2.66**	**0.9776**	**0.00643**	***
Direction	Summer	0.66	0.6868	0.33332	
Direction	**Fall**	**-1.72**	**0.8120**	**0.03426**	**
Frequency	Winter	-2.65	3.4053	0.43604	
Frequency	**Spring**	**-7.92**	**3.6776**	**0.03123**	**
Frequency	**Summer**	**-10.84**	**2.6871**	**0.00006**	***
Frequency	Fall	6.24	5.0793	0.21957	

6 Discussion

6.1 Abiotic Drivers

Storms

This analysis indicates that the annual number of storms in the Palmer region is significantly decreasing over time in the south coastal area as well as during the winter for the entire PAL grid. The number of storms appears to have an increasing trend in the summer and fall but the trend was not statistically significant ($p=0.6$). The slight but insignificant increase in storms in summer and fall could be due to the shortening sea ice season duration which may allow for storms to more easily move across the ocean atmosphere boundary without being impeded by the sea ice. This hypothesis will require a reanalysis of the data with Type II regressions due to the uncertainty of the direction of causality. Spatially, the intensity of storms decreases from offshore to inland. The seasonal differences in intensity are statistically significant. The intensity of storms also did not have a significant linear temporal trend except for a very small increase in winter storm intensity. Climate change is predicted to increase storminess through increased intensity of winds (Montes Hugo et al., 2009) and therefore further analysis is needed to understand why this trend is not apparent. This may be due to the PAL LTER grid being a relatively small region with a short time period for the study from a climate perspective, which means that the natural climate variability is large and likely dominates any climate change signal. Storm duration fluctuates widely with a high standard deviation at around 9.6 hours +/- 6.6 hours; however, storm duration and direction do not change over time. Storm direction does not have a correlation over time either. The storm approach the Palmer study area at an average direction of 115^{o} (or ESE). When analyzing seasonal storm trends, winter does exhibit a slight southward change (0.12^{o}/yr) in storm direction over time, maybe due to changes in ENSO patterns and should be investigated further. The north and south regions of the Palmer study area experience similar mean storm direction whereas the far south has an average difference of -14^{o} (more eastward). The coastal and shelf areas are also statistically similar in storm direction, whereas the slope experiences $+10^{o}$ to 13^{o} (more southward).

Sea Ice

The coastal sites most often exhibit a positive correlation of sea-ice advance with time, indicating that these areas are experiencing later advancement of sea ice. These areas

experienced the majority of significant decreases in the duration of the sea ice season. The Far South also had the most number of significant relationships. Therefore, the Far South and all coastal sites should be investigated further to determine any covariates that could be contributing to the changes. Sea ice interactions suggest that when advance occurs later, the retreat will occur earlier. The authors hypothesize that a later sea-ice advance does not allow for as much sea ice buildup and therefore the weaker sea ice will retreat faster.

Snow

The snow depth shows both variability from annually as well as seasonally. Each season has a statistically different mean snow depth. Snow depth is changing over time for each season. During the winter and fall, the amount of snow is decreasing over time whereas the amount of snow is increasing over the time during the spring and summer. The decrease in winter snow depth coincides with the decrease in frequency of winter storms.

Influence of Storms on Sea Ice and Snow

Correlations of storm frequency with sea ice indices were only found with day of retreat for the northern region overall, north coastal zone, and far south coastal zone. The positive correlation between storm frequency and sea-ice retreat was unexpected as literature shows that storms can cause ice breakup, while these results indicate that more frequent storms would cause a later retreat date. No correlations were found between storm frequency and advance or duration of the sea ice season. The relationship between sea ice and storm intensity varies spatially. The only sub region that has a significant correlation with mean storm intensity was the coastal zone. The predominant index that has a relationship with storms is advancement of sea ice, therefore storms may be impacting the formation of sea ice when higher intensities of storms are reached. The later advancement date in coastal sites could indicate that the storms in that area are reducing the sea ice extent earlier when stronger storms are present. There were no significant findings when investigating the influence of storm direction and duration on sea ice indices. Storm characteristics were used in linear models to predict the timing of sea-ice advance, retreat, and duration. Sea ice advance was most heavily impacted by storm intensity. Interestingly, the time of year impacted the effect that intensity had on sea-ice advance. Higher intensity of storms in the winter and spring from the previous season cause a later advance day, however stronger intensity during the summer immediately before advance causes an earlier advance day. Sea ice

retreat had a similar relationship in that stronger storms during the summer caused a later retreat, whereas stronger storms in the previous fall caused an earlier retreat. The duration of fall storms also negatively correlated with the timing of retreat. Duration of the sea ice season was impacted by intensity in all seasons with summer intensity lengthening the season and spring, fall, and winter storms shortening the season. Previous studies have found that November snow depth was an important factor in modelling clutch initiation date (Cimino et al. 2019) and therefore was modelled as the response to austral spring storm characteristics. The frequency of storms was the only significant contributor to modelling November snow depth. Further analysis should look at monthly predictors or even at an individual storm levels to better understand the interplay of these pulse dynamics.

6.2 Impact of Storms on CFM

The chick fledging mass (CFM) had seasonal variability and interannual variability, however there were no significant changes to CFM over time. Most years have been within the upper and lower bound of survivorship and non-survivorship. Individual linear models showed that storm intensity, direction, and frequency of storms were negatively correlated with CFM. To investigate the relationship further, multiple regression was performed with annual and seasonal averages of the storm characteristics. On the annual scale, the CFM was lower when the frequency of storms increased. This could indicate that the breeding pairs are impacted by the frequency of storms and may not have as favorable conditions in this crucial pre-breeding period. Further analysis should incorporate data from other aspects of penguin phenology to tease out this annual relationship.

Seasonal averages showed a more detailed picture of storm characteristics that may be impacting CFM. Fledglings hatch during the summer and therefore, summer storms would co-occur with the time period in which the adults are feeding the chicks with quality prey to boost their mass. The intensity of spring storms decreases the CFM by up to 57 grams. Conversely, the summer intensity is again opposite of the other months and actually increases the chick weight in the summer (+78 g). However, not all summer storms have a positive correlation. The duration of summer storms can decrease the CFM by almost the same amount (- 70 g). The summer storms could be bringing in new food sources and thus bolstering the CFM. However, there are

many other mechanics at play and an improved upon model could help postulate on why there is discrepancy between summer intensity influence compared to the rest of the year.

7 Conclusion and Future Directions

Storms within the Palmer region have variable spatial patterns for temporal trends as well for correlations with other variables. Winter storms exhibit the only increase in frequency and coastal areas experience the most amount of change in intensity and frequency over time. There are regional and zonal differences amongst characteristics with some areas experiencing little to no change over time. Sea ice is advancing later and is correlated with increased storm intensity. On the other hand, retreat is correlated with increased frequency of storms. Adélie CFM is negatively correlated with storm intensity, frequency, and duration. However, when looking at the compounding relationships and at seasonal scales, the relationships become murky, warranting further investigation into the differences of seasonal influence.

Future work should incorporate a metric for ENSO and SAM to account for the natural climate variability in influencing the sea ice indices and storm direction in particular. An extension of this study could include storms from a wider area due to the potential of larger cyclonic activity coming through the study region (radii of up to 2000 km). In order to enhance current models of CFM, other parameters should be added such as sea ice indices, sea surface temperature, and large scale climate indices as mentioned above. Other penguin metrics could be tracking the influence of storms such as breeding success or population census. Leveraging this study as a model base will allow more investigation into what is causing the decline in the Adélie penguin population and what may occur in southern regions under projected climate conditions.

8 References

Atkinson A, Hill SL, Pakhomov EA, Siegel V and others (2019) Krill (Euphausia superba) distribution contracts southward during rapid regional warming. Nature Climate Change 9:142-147

Boersma PD, Rebstock GA (2014) Climate change increases reproductive failure in Magellanic penguins. PLoS One 9:e85602-e85602

Brown, M.S., Munro, D.R., Feehan, C.J. *et al.* Enhanced oceanic CO_2 uptake along the rapidly changing West Antarctic Peninsula. *Nat. Clim. Chang.* **9**, 678–683 (2019). https://doi.org/10.1038/s41558-019-0552-3

Butterworth, B. J., and Miller, S. D., 2016, "Automated underway eddy covariance system for air-sea momentum, heat, and CO2 fluxes in the Southern Ocean". *Journal of Atmospheric and Oceanic Technology*, 33(4), 635–652. https://doi.org/10.1175/jtech-d-15-0156.1

Chapman EW, Hofmann EE, Patterson DL, Ribic CA, Fraser WR (2011) Marine and terrestrial factors affecting Adélie penguin Pygoscelis adeliae chick growth and recruitment off the western Antarctic Peninsula. Marine Ecology Progress Series 436:273-289

Chappell MA, Morgan KR, Souza SL, Bucher TL (1989) Convection and thermoregulation in two Antarctic seabirds. Journal of Comparative Physiology B 159:313-322

Cimino MA, Fraser WR, Patterson-Fraser DL, Saba VS, Oliver MJ (2014) Large-scale climate and local weather drive interannual variability in Adélie penguin chick fledging mass. Marine Ecology Progress Series 513:253-268

Cimino MA, Lynch HJ, Saba VS, Oliver MJ (2016) Projected asymmetric response of Adélie penguins to Antarctic climate change. Scientific Reports 6:28785

Cimino MA, Patterson-Fraser DL, Stammerjohn S, Fraser WR (2019) The interaction between island geomorphology and environmental parameters drives Adélie penguin breeding phenology on neighboring islands near Palmer Station, Antarctica. Ecology and Evolution 9:9334-9349

Copernicus Climate Change Service (C3S) (2017): ERA5: Fifth generation of ECMWF atmospheric reanalyses of the global climate. Copernicus Climate Change Service Climate Data Store (CDS), date of access. https://cds.climate.copernicus.eu/cdsapp#!/home

DeVries, T., 2014, "The oceanic anthropogenic CO2 sink: storage, air-sea fluxes, and transports

over the industrial era", *Glob. Biogeochem. Cycles* 28, 631–647. doi: 10.1002/2013gb004739

Ducklow HW, Fraser W, Karl DM, Quetin LB and others (2006) Water-column processes in the West Antarctic Peninsula and the Ross Sea: Interannual variations and foodweb structure. Deep Sea Research Part II: Topical Studies in Oceanography 53:834-852

Ducklow H.W., K. Baker, D.G. Martinson, L.B. Quetin, R.M. Ross, R.C. Smith, S.E. Stammerjohn, M. Vernet, W.R. Fraser, 2007, "Marine pelagic ecosystems: the West Antarctic Peninsula", *Phil. Trans. Roy. Soc. Lond. B Biol. Sci*., B362, pp. 67-94.

Ducklow HW, Fraser WR, Meredith MP, Stammerjohn SE and others (2013) West Antarctic Peninsula: An Ice-Dependent Coastal Marine Ecosystem in Transition. Oceanography 26:190-203

Eayrs, C., Li, X., Raphael, M.N. *et al.*, 2021, "Rapid decline in Antarctic sea ice in recent years hints at future change", *Nat. Geosci.* 14, 460–464. https://doi.org/10.1038/s41561-021-00768-3

Fletcher, S. E. M., Gruber, N., Jacobson, A. R., Doney, S. C., Dutkiewicz, S., Gerber, M., et al., 2006, "Inverse estimates of anthropogenic CO2 uptake, transport, and storage by the ocean", *Glob. Biogeochem. Cycles* 20:GB2002.

Fountain AG, Saba G, Adams B, Doran P and others (2016) The Impact of a Large-Scale Climate Event on Antarctic Ecosystem Processes. BioScience 66:848-863

Fraser WR, Patterson-Fraser DL, Ribic CA, Schofield O, Ducklow H (2013) A Nonmarine Source of Variability in Adélie Penguin Demography. Oceanography 26:207-209

Grise KM, Son S-W, Gyakum JR (2013) Intraseasonal and Interannual Variability in North American Storm Tracks and Its Relationship to Equatorial Pacific Variability. Monthly Weather Review 141:3610-3625

Grise, K.M., Son, S.-W., Correa, G.J.P. and Polvani, L.M. (2014), The response of extratropical cyclones in the Southern Hemisphere to stratospheric ozone depletion in the 20th century. Atmos. Sci. Lett., 15: 29-36. https://doi.org/10.1002/asl2.458

Gruber N, Boyd PW, Frolicher TL, Vogt M. 2021. Biogeochemical extremes and compound events in the ocean. Nature 600:395-407

Harris RMB, Beaumont LJ, Vance TR, Tozer CR and others (2018) Biological responses to the press and pulse of climate trends and extreme events. Nature Climate Change 8:579-587

Heinze C, Blenckner T, Martins H, and others. 2020. The quiet crossing of ocean tipping points. Proceedings of the National Academy of Sciences 118(9): e2008478118 doi:10.1073/pnas.2008478118/

Hobbs, W., Massom, R., Stammerjohn, S., Reid, P., Williams, G., Meier, W., 2016 "A review of recent changes in Southern Ocean sea ice, their drivers and forcings," *Global and Planetary Change* 143:228-250

Holland PR, Bracegirdle TJ, Dutrieux P, Jenkins A, Steig EJ (2019) West Antarctic ice loss influenced by internal climate variability and anthropogenic forcing. Nature Geoscience 12:718-724

Hoskins, B.J., Hodges, K.I., 2005 "A New Perspective on Southern Hemisphere Storm Tracks", *Journal of Climate* 18:4108-4129

IPCC, 2021: Summary for Policymakers. In: Climate Change 2021: The Physical Science Basis. Contribution of Working Group I to the Sixth Assessment Report of the Intergovernmental Panel on Climate Change [Masson-Delmotte, V., P. Zhai, A. Pirani, S. L. Connors, C. Péan, S. Berger, N. Caud, Y. Chen, L. Goldfarb, M. I. Gomis, M. Huang, K. Leitzell, E. Lonnoy, J.B.R. Matthews, T. K. Maycock, T. Waterfield, O. Yelekçi, R. Yu and B. Zhou (eds.)]. Cambridge University Press.

Jena, B., Bajish, C.C., Turner, J. *et al.* "Record low sea ice extent in the Weddell Sea, Antarctica in April/May 2019 driven by intense and explosive polar cyclones". *npj Clim Atmos Sci* **5,** 19 (2022). https://doi.org/10.1038/s41612-022-00243-9

Kavanaugh MT, Abdala FN, Ducklow H, Glover D and others (2015) Effect of continental shelf canyons on phytoplankton biomass and community composition along the western Antarctic Peninsula. Marine Ecology Progress Series 524:11-26

Kohout, A., Williams, M., Dean, S. et al., 2014, "Storm-induced sea ice breakup and the implications for ice extent", *Nature* 509, 604–607. https://doi.org/10.1038/nature13262

Marshall, J., Speer K., 2012, "Closure of the meridional overturning circulation through Southern Ocean upwelling", *Nat. Geosci*. 5, 171–180.

Massom, R.A., Scambos, T.A., Bennetts, L.G. *et al.*, 2018, "Antarctic ice shelf disintegration triggered by sea ice loss and ocean swell", *Nature.* **558,** 383–389. https://doi.org/10.1038/s41586-018-0212-1

McClintock J, Ducklow H, Fraser W (2008) Ecological Responses to Climate Change on the

Antarctic Peninsula: The Peninsula is an icy world that's warming faster than anywhere else on Earth, threatening a rich but delicate biological community. American Scientist 96:302- 310

Meehl, G. A. et al., 2019, “Sustained ocean changes contributed to sudden Antarctic sea ice retreat in late 2016”, *Nat. Commun.* 10, 14.

Meehl, G. A., Arblaster, J. M., Bitz, C. M., Chung, C. T. Y., & Teng, H., 2016, “Antarctic sea ice expansion between 2000 and 2014 driven by tropical Pacific decadal climate variability”, *Nat. Geo*. **9**, 590–595.

Montes-Hugo M, Doney SC, Ducklow HW, Fraser W, Martinson D, Stammerjohn SE, Schofield O (2009) Recent Changes in Phytoplankton Communities Associated with Rapid Regional Climate Change Along the Western Antarctic Peninsula. Science 323:1470-1473

Palmer LTER NSF Project Summary 2022

Palmer Station Antarctica LTER, M. Cimino, and W. Fraser. 2022. Adelie penguin chick fledging weights, 1991-2021 ver 7. Environmental Data Initiative. https://doi.org/10.6073/pasta/875086ecf38755f29f7aa8209e839e7f (Accessed 2022-10-29).

Palmer Station Antarctica LTER, M. Cimino, and W. Fraser. 2022. Adelie penguin reproduction success, 1991-2021 ver 7. Environmental Data Initiative. https://doi.org/10.6073/pasta/cb20f29bb1113e986bfcff8873f7de97 (Accessed 2022-10-29).

Palmer Station Antarctica LTER and S. Stammerjohn. 2020. Sea ice duration or the time elapse between day of advance and day of retreat within a given sea ice year for the PAL LTER region West of the Antarctic Peninsula derived from passive microwave satellite, 1978 - 2019. ver 6. Environmental Data Initiative. https://doi.org/10.6073/pasta/c9f43e1f01ade7e2a56f765a8d79bbd3 (Accessed 2022-03-22).

Parkinson, C. L., 2019, “A 40-y record reveals gradual Antarctic sea ice increases followed by decreases at rates far exceeding the rates seen in the Arctic”, *Proc. Natl Acad. Sci. USA* **116**, 14414–14423.

Patterson DL, Easter-Pilcher A, Fraser W (2003) The effects of human activity and

environmental variability on long-term changes in Adelie penguin populations at Palmer Station Antarctica. In: Huiskes AHL, Gieskes WWC, Rozema J, R.M.L. S, van der vies SM, Wolff WJ (eds) Antarctic Biology in a Global Context. Backhuys Publishers, Leiden

Poloczanska ES, Brown CJ, Sydeman WJ, Kiessling W and others (2013) Global imprint of climate change on marine life. Nature Climate Change 3:919-925

Orr, J. C., Maier-Reimer, E., Mikolajewicz, U., Monfray, P., Sarmiento, J. L., Toggweiler, J. R., et al., 2001, "Estimates of anthropogenic carbon uptake from four three-dimensional global ocean models", *Glob. Biogeochem. Cycles* 15, 43–60. doi: 10.1029/2000gb001273

Reguero, B.G., Losada, I.J. & Méndez, F.J. (2019). A recent increase in global wave power as a consequence of oceanic warming. Nature Communications, 10, 205. https://doi.org/10.1038/s41467-018-08066-0

Saba GK, Fraser WR, Saba VS, Iannuzzi RA and others (2014) Winter and spring controls on the summer food web of the coastal West Antarctic Peninsula. Nature Communications 5:4318

Schofield O, Ducklow HW, Martinson DG, Meredith MP, Moline MA, Fraser WR (2010) How Do Polar Marine Ecosystems Respond to Rapid Climate Change? Science 328:1520-1523

Schofield O, Saba G, Coleman K, Carvalho F and others (2017) Decadal variability in coastal phytoplankton community composition in a changing West Antarctic Peninsula. Deep Sea Research Part I: Oceanographic Research Papers 124:42-54

Schofield O, Brown M, Kohut J, Nardelli S, Saba G, Waite N, Ducklow H (2018) Changes in the upper ocean mixed layer and phytoplankton productivity along the West Antarctic Peninsula. Philosophical Transactions of the Royal Society A: Mathematical, Physical and Engineering Sciences 376:20170173

Schultz, C., Doney, S. C., Zhang, W. G., Regan, H., Holland, P., Meredith, M. P., & Stammerjohn, S. (2020). Modeling of the influence of sea ice cycle and Langmuir circulation on the upper ocean mixed layer depth and freshwater distribution at the West Antarctic Peninsula. Journal of Geophysical Research: Oceans, 125, e2020JC016109. https://doi.org/10.1029/2020JC016109

Shadwick, E. H., De Meo, O. A., Schroeter, S., Arroyo, M. C., Martinson, D. G., & Ducklow,

H., 2021, “Sea ice suppression of CO2 outgassing in the West Antarctic Peninsula: Implications for the evolving Southern Ocean carbon sink”, *Geophysical Research Letters, 48,* e2020GL091835. https://doi. org/10.1029/2020GL091835

Smith MD (2011) An ecological perspective on extreme climatic events: a synthetic definition and framework to guide future research. Journal of Ecology 99:656-663

Stammerjohn, S., Maksym, T., Heil, P., Massom, R., Vancoppenolle, M., Leonard, K., 2011 “The influence of winds, sea-surface temperature and precipitation anomalies on Antarctic regional sea ice conditions during IPY 2007”, Deep Sea Research Part II: Topical Studies in Oceanography 58:999-1018

Stammerjohn, S., Massom, R., Rind, D., & Martinson, D., 2012, “Regions of rapid sea ice change: An inter-hemispheric seasonal comparison”, *Geophysical Research Letters*, 39(6), 1–8. https://doi.org/10.1029/2012GL050874

Stammerjohn S, Maksym T (2017) Gaining (and losing) Antarctic sea ice: Variability, trends and mechanisms. In: Thomas DN (ed) Sea Ice. John Wiley & Sons, Ltd, West Sussex p. 261-289.

Stammerjohn, S., Martinson, D., Smith, R., Yuan, X., Rind, D., 2008 “Trends in Antarctic annual sea-ice retreat and advance and their relation to El Niño–Southern Oscillation and Southern Annular Mode variability”, *Journal of Geophysical Research*: Oceans 113. doi.org/10.1029/2007JC004269

Stammerjohn SE, Scambos TA. 2020. Warming reaches the South Pole. Nature Climate Change 10:710-711.doi:10.1038/s41558-020-0827-8

Steinberg DK, Ruck KE, Gleiber MR, Garzio LM and others (2015) Long-term (1993–2013) changes in macrozooplankton off the Western Antarctic Peninsula. Deep Sea Research Part I: Oceanographic Research Papers 101:54-70

Thibault KM, Brown JH (2008) Impact of an extreme climatic event on community assembly. Proceedings of the National Academy of Sciences 105:3410-3415

Wang, J., Luo, H., Yang, Q. *et al.* An Unprecedented Record Low Antarctic Sea ice Extent during Austral Summer 2022. *Adv. Atmos. Sci.* **39**, 1591–1597 (2022). https://doi.org/10.1007/s00376-022-2087-1

Weiss, R. F., 1974, “Carbon dioxide in water and seawater: The solubility of a non-ideal gas”, *Marine Chemistry*, 2(3), 203–215. https://doi.org/10.1016/0304-4203(74)90015-2

Wernberg T, Bennett S, Babcock RC, de Bettignies T and others (2016) Climate-driven regime shift of a temperate marine ecosystem. Science 353:169-172

Yang, B., E.H. Shadwick, C. Schultz, and S.C. Doney, 2021: Annual mixed layer carbon budget for the West Antarctic Peninsula continental shelf: Insights from year-round mooring measurements, J. Geophys. Res. Oceans, 126, e2020JC016920, https://doi.org/10.1029/2020JC016920

Young IR, Ribal A. (2019). Multiplatform evaluation of global trends in wind speed and wave height. Science, 364(6440), eaav9527. https://doi.org/10.1126/science.aav9527

Young IR, Sanina E, Babanin AV. (2017). Calibration and Cross Validation of a Global Wind and Wave Database of Altimeter, Radiometer, and Scatterometer Measurements. Journal of Atmospheric and Oceanic Technology, 34(6), 1285–1306. https://doi.org/10.1175/jtech-d-16- 0145.1

Young IR, Zieger S, Babanin AV (2011). Global Trends in Wind Speed and Wave Height. Science, 332(6028), 451–455. https://doi.org/10.1126/science.1197219

Yuan X, Kaplan MR, Cane MA (2018) The Interconnected Global Climate System—A Review of Tropical–Polar Teleconnections. Journal of Climate 31:5765-5792

Zuur, A., Ieno, E. N., Walker, N., Saveliev, A. A., & Smith, G. M. (2009). Mixed effects models and extensions in ecology with R (2009th ed.). Springer.